


## RESEARCH ARTICLE

# Photochemical sensitivity to emissions and local meteorology in Bogotá, Santiago, and São Paulo: An analysis of the initial COVID-19 lockdowns

Rodrigo J. Seguel<sup>1,2,\*</sup> , Laura Gallardo<sup>1,2</sup>, Mauricio Osses<sup>1,3</sup>, Néstor Y. Rojas<sup>4</sup>, Thiago Nogueira<sup>5</sup>, Camilo Menares<sup>1,2</sup>, Maria de Fatima Andrade<sup>5</sup>, Luis C. Belalcázar<sup>4</sup>, Paula Carrasco<sup>2</sup>, Henk Eskes<sup>6</sup>, Zoë L. Fleming<sup>1,7</sup>, Nicolas Huneus<sup>1,2</sup>, Sergio Ibarra-Espinosa<sup>5</sup>, Eduardo Landulfo<sup>8</sup>, Manuel Leiva<sup>9</sup>, Sonia C. Mangones<sup>10</sup>, Fernando G. Morais<sup>8</sup>, Gregori A. Moreira<sup>11</sup>, Nicolás Pantoja<sup>3</sup>, Santiago Parraguez<sup>1,12</sup>, Jhojan P. Rojas<sup>13</sup>, Roberto Rondanelli<sup>1,2</sup>, Izabel da Silva Andrade<sup>8</sup>, Richard Toro<sup>9</sup>, and Alexandre C. Yoshida<sup>8,14,15</sup>

This study delves into the photochemical atmospheric changes reported globally during the pandemic by analyzing the change in emissions from mobile sources and the contribution of local meteorology to ozone (O<sub>3</sub>) and particle formation in Bogotá (Colombia), Santiago (Chile), and São Paulo (Brazil). The impact of mobility reductions (50%–80%) produced by the early coronavirus-imposed lockdown was assessed through high-resolution vehicular emission inventories, surface measurements, aerosol optical depth and size, and satellite observations of tropospheric nitrogen dioxide (NO<sub>2</sub>) columns. A generalized additive model (GAM) technique was also used to separate the local meteorology and urban patterns from other drivers relevant for O<sub>3</sub> and NO<sub>2</sub> formation. Volatile organic compounds, nitrogen oxides (NO<sub>x</sub>), and fine particulate matter (PM<sub>2.5</sub>) decreased significantly due to motorized trip reductions. In situ nitrogen oxide median surface mixing ratios declined by 70%, 67%, and 67% in Bogotá, Santiago, and São Paulo, respectively. NO<sub>2</sub> column medians from satellite observations decreased by 40%, 35%, and 47%, respectively, which was consistent with the changes in mobility and surface mixing ratio reductions of 34%, 25%, and 34%. However, the ambient NO<sub>2</sub> to NO<sub>x</sub> ratio increased, denoting a shift of the O<sub>3</sub> formation regime that led to a 51%, 36%, and 30% increase in the median O<sub>3</sub> surface mixing ratios in the 3 respective cities. O<sub>3</sub> showed high sensitivity to slight temperature changes during the pandemic lockdown period analyzed. However, the GAM results indicate that O<sub>3</sub> increases were mainly caused by emission changes. The lockdown led to an increase in the median of the maximum daily 8-h average O<sub>3</sub> of between 56% and 90% in these cities.

**Keywords:** Ozone, Nitrogen oxides, Mobile sources, Lockdown, Generalized additive model

<sup>1</sup>Center for Climate and Resilience Research (CR)<sup>2</sup>, Santiago, Chile

<sup>2</sup>Department of Geophysics, Faculty of Physical and Mathematical Sciences, University of Chile, Santiago, Chile

<sup>3</sup>Departamento Ingeniería Mecánica, Universidad Técnica Federico Santa María (UTFSM), Santiago, Chile

<sup>4</sup>Department of Chemical and Environmental Engineering, Universidad Nacional de Colombia, Bogotá, Colombia

<sup>5</sup>Departamento de Ciências Atmosféricas, Instituto de Astronomia, Geofísica e Ciências Atmosféricas, Universidade de São Paulo, São Paulo, Brazil

<sup>6</sup>Royal Netherlands Meteorological Institute (KNMI), De Bilt, the Netherlands

<sup>7</sup>Envirohealth Dynamics Lab, C+ Research Center in Technologies for Society, School of Engineering, Universidad Del Desarrollo, Santiago, Chile

<sup>8</sup>Institute for Energy and Nuclear Research, São Paulo, Brazil

<sup>9</sup>Department of Chemistry, Faculty of Science, University of Chile, Santiago, Chile

<sup>10</sup>Department of Civil and Agricultural Engineering, Universidad Nacional de Colombia, Bogotá, Colombia

<sup>11</sup>Federal Institute of São Paulo, São Paulo, Brazil

<sup>12</sup>Department of Mechanical Engineering, Faculty of Physical and Mathematical Sciences, University of Chile, Santiago, Chile

<sup>13</sup>National Meteorology and Hydrology Service (SENAMHI), Lima, Peru

<sup>14</sup>Instituto de Física da Universidade de São Paulo, São Paulo, Brazil

<sup>15</sup>Instituto de Ciências Exatas e Naturais do Pontal, Universidade Federal de Uberlândia, Ituiutaba, Minas Gerais, Brazil

\*Corresponding author:  
Email: [rodrigoseguel@uchile.cl](mailto:rodrigoseguel@uchile.cl)

## 1. Introduction

Nearly 85% of South America's population lives in urban areas (United Nations, 2019), which, combined with extreme social, economic, and environmental segregation (e.g., Romero et al., 2012; Carpenter and Quispe-Agnoli, 2015; Guzmán and Bocarejo, 2017), makes these cities highly vulnerable to air pollution and climate change (Garschagen and Romero-Lankao, 2015). Bogotá, Santiago, and São Paulo together have ca. 40 million inhabitants and increasing motorization rates (**Table 1**). Mobile sources have contributed to air pollution and its evolution in these cities in recent decades (e.g., Nogueira et al., 2015; de Andrade et al., 2017; Barraza et al., 2017; Gallardo et al., 2018; Seguel et al., 2020; East et al., 2021). Emissions from mobile sources depend on the intertwined effects of changes in mobility, land use, population and economic growth, vehicle technology, decision making, and urban governance (e.g., Kelly and Zhu, 2016; Javaid et al., 2020). Despite technological advances that have led to notable reductions in pollutant and greenhouse gas emissions per vehicle and the implementation of vehicle restriction plans, attainment plans, and boosting public transport, motor vehicles—in and around our cities—are still a strong driver of pollutants and climate forcers. This, in turn, affects air composition and the quality of life of citizens.

It is well known that while primary pollution responds largely linearly to changes in emissions, secondary pollution is a nonlinear process (e.g., Parrish et al., 1999). Ozone ( $O_3$ ) and secondary aerosols are initiated from the oxidation of volatile organic compounds (VOCs) by hydroxyl radicals (OH; e.g., Andreae and Crutzen, 1997). This mechanism involves the net production of nitrogen dioxide ( $NO_2$ ), whose photolysis produces  $O_3$ . Additionally, as oxidation proceeds, the typically high vapor pressures of primary VOCs decrease, favoring partitioning into the aerosol phase (e.g., Goldstein and Galbally, 2007). The VOC to  $NO_x$  ratio (VOC/ $NO_x$ ) is fundamental to the understanding of the nonlinear photochemistry of  $O_3$  because it reflects the competition of VOCs and  $NO_x$  for OH (Fujita et al., 2003). In urban atmospheres with typically high levels of  $NO_x$  (VOC-limited), the formation of nitric acid represents the dominant radical sink, in which  $NO_2$  removes OH, while NO titrates  $O_3$ . Under this regime, reductions in  $NO_x$  must be accompanied by comparable or greater reductions in

VOCs to prevent the increase in  $O_3$  formed via VOC oxidation. The shifts in  $O_3$  formation regimes from relatively low to high VOC/ $NO_x$  have been observed in Santiago and (central) São Paulo (Silva Júnior et al., 2009; Seguel et al., 2012). In these cities, higher levels of  $O_3$  are frequently measured during the weekends when  $NO_x$  levels are lower compared with weekdays. Conversely, increases in  $NO_x$  may result in decreases in  $O_3$ , which were noted in urban areas of São Paulo between 2009 and 2011, when higher ethanol prices induced 2 million drivers in São Paulo to switch to using gasoline (Vara-Vela et al., 2016; Schuch et al., 2019). The resulting increase in  $NO_x$  emissions resulted in up to 30% decreases in  $O_3$  concentrations (Salvo and Geiger, 2014); however, the emission of ultrafine particles also rose by the same magnitude (Salvo et al., 2017).

The global COVID-19 outbreak in 2020 led to significant declines in vehicle emissions as lockdowns were imposed, limiting the use of fossil fuel-powered vehicles (e.g., Kroll et al., 2020; Le et al., 2020). Hence, mobility restrictions modified the VOC/ $NO_x$  ratio, leading to an increase in  $O_3$ , as reported for several cities worldwide (Connerton et al., 2020; Nakada and Urban, 2020; Siciliano et al., 2020; Gkatzelis et al., 2021; Rodríguez-Villamizar et al., 2021; Toro et al., 2021). In several areas, meteorological conditions could nevertheless result in amplification or damping of photochemical effects leading to secondary pollutants (e.g., Le et al., 2020; Ordóñez et al., 2020; Gaubert et al., 2021; Shi et al., 2021).

During the start of the coronavirus pandemic in South America in March–May 2020, adherence to mobility restrictions varied with time as well as between and within cities. There was generally less adherence in poorer communes, where household income depends on daily activities typically carried out far from home either in informal commerce or in domestic service (Comisión Económica para América Latina y el Caribe/Organización Internacional del Trabajo, 2020). Given that large cities are key to national economies (**Table 1**), governments and economic sectors were reluctant to adopt a complete lockdown, maintaining, in addition to essential activities (food, health, energy, and water provisioning), that the public sector services, banks, and industrial sectors remain open. Notably, in the case of São Paulo, mayor and governor

**Table 1.** Location and population statistics for Bogotá, Santiago, and São Paulo urban agglomerations according to the United Nations (United Nations, 2019) during the lockdown in March–May 2020. DOI: <https://doi.org/10.1525/elementa.2021.00044.t1>

City (Location)	Population	Motor Vehicles	City GDP as Percentage of National GDP	Lockdown Period Analyzed
Bogotá (4.6°N, 74.1°W, 2,600 m a.s.l.)	$1.06 \cdot 10^7$	$2.68 \cdot 10^6$	25.7	March 23–May 23
Santiago (33.5°S, 70.5°W, 500 m a.s.l.)	$7.24 \cdot 10^6$ <sup>a</sup>	$2.20 \cdot 10^6$	42.3	March 26–May 14
São Paulo (23.5°S, 46.7°W, 740 m a.s.l.)	$2.17 \cdot 10^7$	$7.28 \cdot 10^6$	33.7	March 24–May 23

The annual city gross domestic product (GDP) is also included as a percentage of the annual national GDP for the year 2016 (<https://estadisticas.cepal.org/cepalstat/Portada.html>).

<sup>a</sup>For Santiago, the estimate of affected people in city districts is based on the latest census (Instituto Nacional de Estadísticas, 2017).

decisions were largely counteracted by the federal government (The Lancet, 2020), leading to less adherence.

In this study, we investigated the changes in emissions from mobile sources that were modified by COVID-19 lockdowns in 3 South American cities: Bogotá (Colombia), Santiago (Chile), and São Paulo (Brazil). We focused on the impacts of the changes in primary and secondary air pollutants and the resulting local photochemistry. To accomplish this goal, we analyzed data from high-resolution vehicular emission inventories and in situ and remote observations to characterize the changes in mobile emissions and air quality compared with previous years (2014–2019) for all 3 cities. Additionally, we used a generalized additive model (GAM) technique to disentangle the roles of local meteorology, day of the week, and seasonality from other drivers of O<sub>3</sub> and NO<sub>2</sub> changes in these megacities. Thus, by analyzing commonalities and differences among Bogotá, Santiago, and São Paulo, we aim to provide a more systemic perspective to address photochemical air pollution in complex and diverse urban environments and its sensitivity to emissions and local meteorology. This is particularly important in terms of developing efficient air quality and climate policies for our cities in the near future.

## 2. Data and methodology

### 2.1. Traffic counts and motor vehicle emissions

Nonmethane VOC (hereafter referred to as VOCs), NO, NO<sub>2</sub>, PM<sub>2.5</sub>, and CO emissions were estimated through state-of-the-science vehicular emission models for Bogotá, Santiago, and São Paulo. Emission factors were generally adapted from the COmputer Programme to calculate Emissions from Road Transport of the European Environment Agency, considering actual fleet technology, fuel quality, environmental conditions, and vehicle activity in Bogotá, Santiago, and São Paulo.

In Bogotá, traffic activity data were derived from a static macroscopic transport model, reflecting Bogotá's morning rush hour traffic conditions in 2015 (Mangones et al., 2019). Traffic changes during lockdown were estimated based on manual traffic counts in 10 arterial-road intersections in Bogotá from April 20 to May 1, 2020. Further details of traffic counts and data sources can be found in Table S1.

For Santiago, reference traffic activity was based on vehicular flow data for the 2011–2015 period, including origin-destination information for 45 communes in the metropolitan area of Santiago. The effect of lockdown strategies on vehicle traffic for the March–April 2020 period was obtained from the Tomtom traffic index ([https://www.tomtom.com/en\\_gb/traffic-index/](https://www.tomtom.com/en_gb/traffic-index/)). Additionally, information from the Operational Transit Control Unit was considered (Table S1), comprising 49 traffic-count stations from 5 communes, for the periods between March 2 and 8 (before COVID-19 restrictions) and between March 30 and April 5, 2020 (during lockdown restrictions).

In the metropolitan area of São Paulo, vehicle activity (Table S1) and emissions were estimated using the Vehicular Emissions Inventories model (Ibarra-Espinosa et al., 2018; 2020). Hourly traffic counts were aggregated for several types of vehicles from toll stations in São Paulo

for March 2020. The lockdown period was defined as March 23–28, and March 2–8 was denoted prelockdown.

### 2.2. In situ observations

We analyzed 4 monitoring stations in Bogotá, 8 in Santiago, and 5 in São Paulo to characterize the impact of emission changes during the variety of measures implemented to decrease the spread of COVID-19 in early 2020 (for simplicity, hereafter referred to as lockdown). The lockdown period in Bogotá was affected by the transport of biomass-burning pollution from Venezuela and the Colombian eastern plains during March (Mendez-Espinosa et al., 2019; **Table 1**). During the Santiago and São Paulo lockdown periods, the photochemistry was still strong enough to provide insights into the chemical mechanisms controlling secondary pollutant formation.

In Santiago, 3 of the 8 stations studied were located in an area under lockdown over the whole period. The rest of the Metropolitan Region was only under nighttime curfew (22:00–5:00). In São Paulo, the selected sites ranged from suburban-scale (outskirts of the city) to urban-scale stations. The locations of the stations are shown in **Table 2** (see also Figure S3), and Table S2 provides more details of each monitoring station.

The air quality networks of Bogotá, Santiago, and São Paulo use instrumentation that complies with U.S. Environmental Protection Agency (EPA) reference methods. The time series used in this study was validated by each national Environmental Agency according to their own protocols. In some cases, preliminary data were used, which were validated after several checks that included completeness, instrument detection limits, revision of isolated extremely high hourly values, and other statistical analyses.

In each city, we defined the baseline period as a (2014–2019) multiyear average of pollutant concentrations. The lockdown period, when mobility restrictions were enforced, was defined as March 23–May 23 in Bogotá, March 16–May 14 in Santiago, and March 24–May 23 in São Paulo. The lockdown periods of each city were compared with the same periods of the baseline. This analysis was carried out with hourly data (air pollutants and meteorological parameters) whose periods had more than 70% validated data for every year at each station. The metrics used for statistical analysis were based on daily means and the maximum daily 8-h average (MDA8).

### 2.3. NO<sub>2</sub> tropospheric column

We used NO<sub>2</sub> tropospheric column observations obtained by the Tropospheric Monitoring Instrument (TROPOMI) onboard the Copernicus Sentinel-5 Precursor (S-5P) platform for the lockdown periods listed in **Table 1**. Descriptions and validations of these data can be found in many studies (e.g., Judd et al., 2020; van Geffen et al., 2020; Verhoelst et al., 2021). The TROPOMI data were cloud filtered, and time averages were produced by mapping the observations to a regular oversampling grid of approximately 2 × 2 km. A suitable approximation for the tropospheric column errors was used to scale linearly with the observations (T Verhoelst, private communications,

**Table 2.** Monitoring stations, their geographical location, and median percentage changes between lockdown and base scenario for CO (ppmv), NO (ppbv), NO<sub>2</sub> (ppbv), O<sub>3</sub> (ppbv), and PM<sub>2.5</sub> (µg m<sup>-3</sup>). DOI: <https://doi.org/10.1525/elementa.2021.00044.t2>

City	Station Name	Latitude (°S)	Longitude (°W)	Altitude (m a.s.l.)	CO	NO	NO <sub>2</sub>	O <sub>3</sub>	PM <sub>2.5</sub>
Bogotá	1. Carvajal–Sevillana (Southwestern Bogotá)	-4.625	74.161	2,553	-43.5	-56.7	-29.0	+53.1	-35.8
	2. Centro de Alto Rendimiento–CDAR (Central Bogotá)	-4.658	74.084	2,548	-31.9	-91.8	-52.1	+67.3	-44.5
	3. Guaymaral (Northeastern Bogotá)	-4.784	74.044	2,557	–	-68.4	-32.7	+28.9	-18.2
	4. Tunal (Southern Bogotá)	-4.576	74.130	2,688	-38.2	-71.0	-35.4	+47.9	-51.5
Santiago	1. Cerro Navia	33.433	70.732	487	-25.5	-67.2	-19.9	+21.5	-12.4
	2. El Bosque	33.547	70.666	567	-8.7	-55.5	-17.1	+33.2	-10.9
	3. Independencia	33.422	70.651	545	+7.4	–	–	+41.2	-15.0
	4. La Florida	33.517	70.588	592	+5.7	-65.8	-11.8	–	-19.6
	5. Las Condes (Eastern Santiago)	33.464	70.661	524	-32.7	-74.0	-43.5	+62.2	-23.9
	6. Parque O'Higgins (Central Santiago)	33.377	70.523	785	-29.2	-60.1	-25.3	+40.8	-18.8
	7. Pudahuel (Western Santiago)	33.438	70.750	478	-14.7	-68.6	-47.0	+35.4	-13.2
	8. Puente alto	33.591	70.594	651	-26.3	-68.2	-37.3	+35.5	-8.0
São Paulo	1. Congonhas (Central CGH SP)	23.616	46.663	760	-42.1	-46.2	-16.6	–	-27.1
	2. Ibirapuera (Park IBI SP)	23.592	46.661	750	-22.7	-66.7	-33.6	+31.0	-29.9
	3. Ponte dos Remedios (Central REM SP)	23.519	46.743	730	-28.4	-44.7	-21.1	–	-20.7
	4. Parque Dom Pedro (Central DP SP)	23.545	46.628	740	-59.9	-68.6	-38.7	+29.9	-7.5
	5. Pinheiros (Central PIN SP)	23.561	46.702	740	-44.5	-73.2	-46.2	+25.5	-8.0

The metric used for CO, NO, NO<sub>2</sub>, and PM<sub>2.5</sub> was the daily mean, and for O<sub>3</sub> was the maximum daily 8-h average.

September 3, 2020). Therefore, relative percentage changes in NO<sub>2</sub>, comparing 2020 with 2019, are reported in this article. It is worth noting that TROPOMI overpass local time is at 13:30, and thus, the columns are not based on a daily average. This is important to keep in mind when NO<sub>2</sub> columns are compared with in situ observations or emission estimates of NO<sub>2</sub>.

#### 2.4. Measured aerosol parameters and estimated secondary aerosols

To further explore the impact of lockdown on atmospheric composition in Santiago and São Paulo, data from the Aerosol Robotic Network (Holben et al., 1998) were examined. The aerosol optical depth (AOD) at 500 nm and the Ångström exponent (AE) during the March 20–April 3, 2020, period in central Santiago (33.458 S, 70.665 W) and March 24–April 15, 2020, at São Paulo University campus (23.561 S, 46.735 W) were compared with a multiyear average of the same dates for 2015–2019.

An empirical method (Chang and Lee, 2007) was used to estimate the fractions of primary and secondary aerosols in the 3 cities. According to this approach, carbon monoxide is used to trace primary combustion sources, while the daily maxima of O<sub>3</sub> (O<sub>3max</sub>) serves as a proxy for the photochemical production of inorganic and organic aerosols. Essentially, the better the PM<sub>2.5</sub>-to-CO correlation is, the more primary aerosols there will be, and the higher the ozone levels are, the more secondary particles there will be. Thus, the primary aerosol fraction is calculated for days when O<sub>3max</sub> does not exceed the background O<sub>3</sub>, and the daily secondary fraction is estimated as the difference between the observed PM<sub>2.5</sub> and the primary fraction. The background O<sub>3</sub> mixing ratio is in turn estimated from the intercept of the regression between O<sub>x</sub> = O<sub>3</sub> + NO<sub>2</sub> and NO<sub>x</sub> during daytime from an upwind station in each city. The methodology was recently applied in Santiago by Menares et al. (2020).

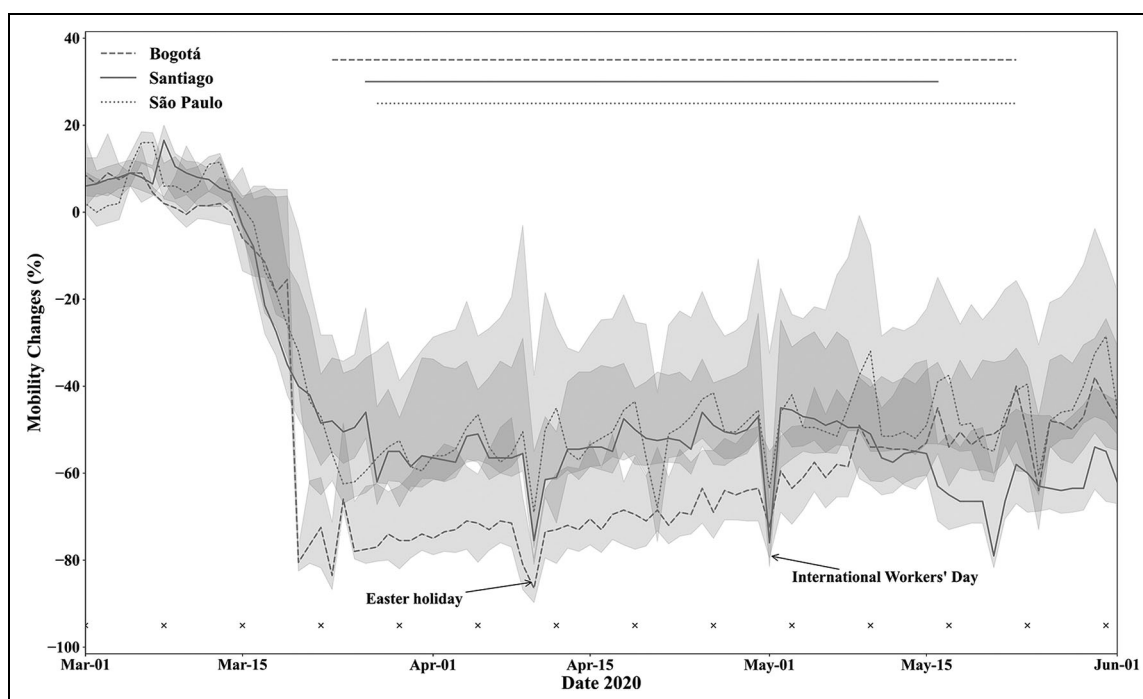


**Figure 1.** Median mobility changes (in percentage) between March and June 2020 in Bogotá (dashed line), Santiago (continuous line), and São Paulo (dotted line) among retail and recreation, commerce, and so on, according to the COVID-19 Community Mobility Report by Google (<https://www.google.com/covid19/mobility/>), on April 20, 2021). The shaded areas show the 0.25 and 0.75 percentiles. This database defines differences in mobility with respect to a period in January 2020. Superimposed, we show the periods of lockdown considered in each city: March 23–May 23 in Bogotá, March 16–May 14 in Santiago, and March 24–May 23 in São Paulo. DOI: <https://doi.org/10.1525/elementa.2021.00044.f1>

### 2.5. Disentangling local meteorology and other factors

GAMs are nonlinear regression tools that allow for nonparametric fittings of complex dependences of response variables, such as  $O_3$  and  $NO_2$ , on explanatory variables, for example, weather, seasonality (Julian day), day of the week, trends, and so on (Ordóñez et al., 2020; Solberg et al., 2021). Thus, a GAM adopts a sum of arbitrary functions of variables—possibly nonlinear—that represent different features via splines, which all together describe the magnitude and variability of the response variables (e.g., Molnar, 2022). The choice of explanatory variables brings in the physics of the problem at hand (e.g., Solberg et al., 2021). Here, we applied expert knowledge, examples from previous applications, and a ranking of variables according to the Akaike information criterion (Cavanaugh and Neath, 2019). Subsequently, we used partial dependence plots (Friedman, 2001) to interpret the model structure and outputs.

A GAM was applied to estimate MDA8 for  $O_3$  and  $NO_2$  with the following input variables recorded by the monitoring stations (Section 2.2): daily maximum temperature ( $^{\circ}C$ ), radiation (in  $W/m^2$ ), wind speed (in  $m/s$ ), and specific humidity (in  $g/kg$ ), as well as the day of the week and the day of the year (Julian day). While the former variables characterize changes in local meteorology, the temporal variables should reflect typical changes in urban activity patterns. Thus, the application of this model to data from the lockdown periods can detect changes due to factors

other than meteorology and typical urban activity. For example, in this case, there were unprecedented changes in mobility and mobile emissions.

## 3. Results and discussion

### 3.1. Emissions

Between March and May 2020, mobility decreased by up to 80% in Bogotá and up to 50%–60% in Santiago and São Paulo, as illustrated in **Figure 1**. The figure illustrates how mobility changes evolved in the 3 cities and the differences between each city, except for when religious festivities coincided between countries. In the following subsections, the impact of mobility restrictions on vehicle emissions and concentrations of primary pollutants are addressed. Note that these estimates are based on local traffic counting and not the database illustrated in **Figure 1**.

#### 3.1.1. Bogotá

Traffic in Bogotá during lockdown decreased for all vehicle types and in all zones. Motorcycles and light-duty vehicle circulation decreased by 53% and 73%, respectively, and urban buses decreased by 40% on average. Small and heavy truck circulation decreased by 58% and 28%, respectively. The only increase in circulation noted was for long-distance buses in the city center, which increased by approximately 39%. These changes in traffic are expected to have been observed only during the mandatory lockdown period in Bogotá. National and local authorities imposed personal

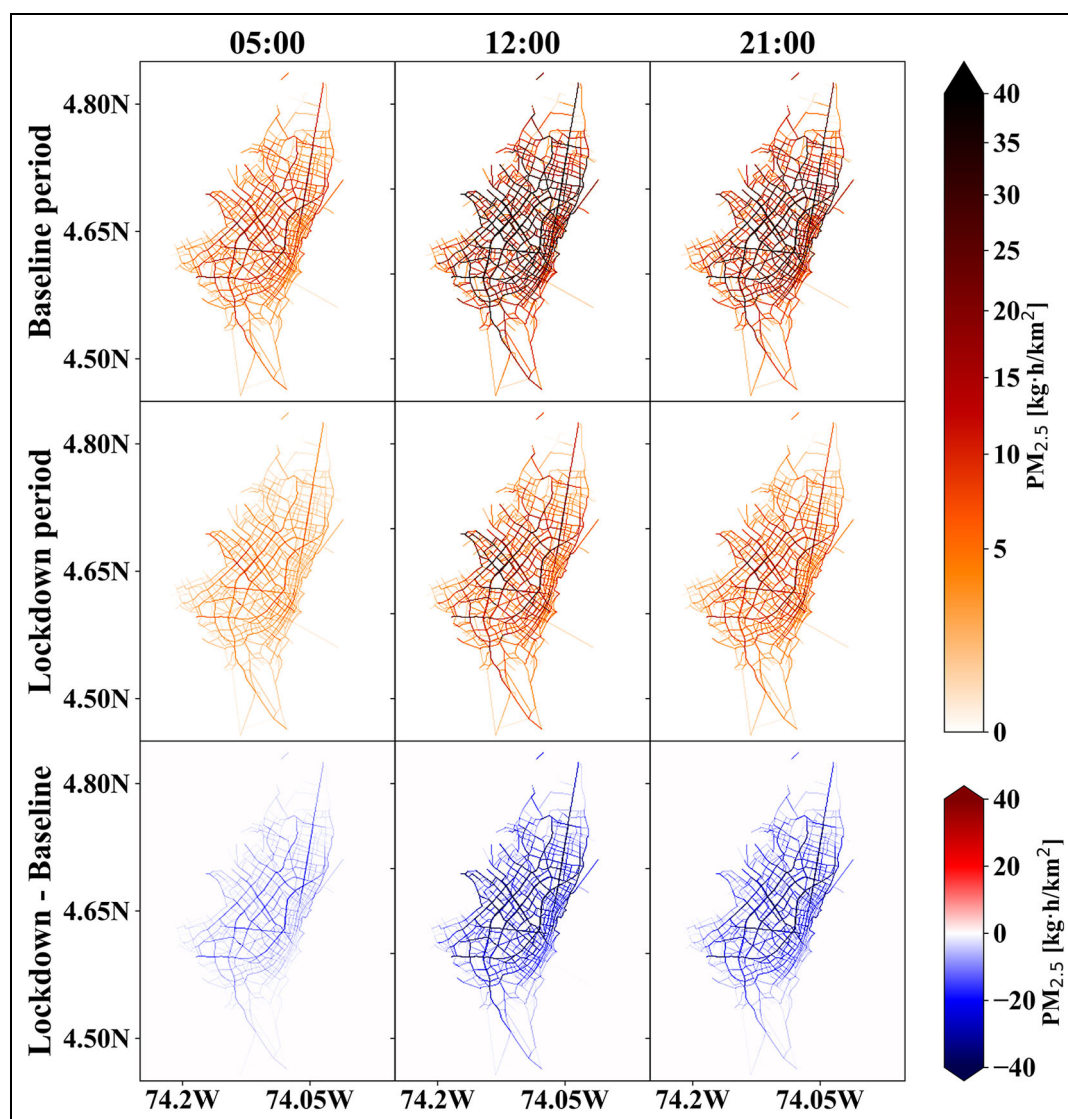


**Figure 2. PM<sub>2.5</sub> vehicle emissions in Bogotá at 3 different hours.** The top panels show the baseline period, the middle panels correspond to the lockdown period (April 20–May 1, 2020), and the bottom panels correspond to the difference in lockdown-baseline emissions. DOI: <https://doi.org/10.1525/elementa.2021.00044.f2>

mobility restrictions and made operational changes in urban and suburban public transport systems.

We estimated that PM<sub>2.5</sub> emissions decreased on average between 77% and 51% across the city during the morning rush hour. NO<sub>x</sub> and VOC decreased by 71%–30% and 73%–54%, respectively. The emission reduction in NO<sub>x</sub> between normal and lockdown conditions was 52.6 t/d, while the emission reduction in VOCs was 30.8 t/d. Light-duty vehicles contributed more strongly to emissions compared with reductions from buses and trucks due to the traffic behavior during lockdown. As shown in **Figure 2**, the city center had a lower PM<sub>2.5</sub> emission decrease rate, reaching a 52% decrease on average during the morning rush hour. The emission reduction rate of PM<sub>2.5</sub> also varied throughout the day, with higher emission reduction rates during morning (5:00–7:00) and evening (19:00–21:00) peak hours than during off-peak hours (0:00–4:00). We attribute this behavior to a greater effect of speed on emissions during high traffic

congestion (rush hour). Alleviating traffic during heavily congested hours allows a greater number of vehicles to increase their speed compared with off-peak hours. **Figure 2** shows PM<sub>2.5</sub> emissions during the baseline and lockdown periods at peak and off-peak hours in Bogotá. NO<sub>x</sub> emission graphs are included as Supplemental Material (Figure S1).

### 3.1.2. Santiago

The analysis of mobility information in Santiago shows a different behavior between areas with mandatory confinement and those in which it was voluntary. Communes with compulsory restrictions (7 of 52) showed a reduction in motorized trips during lockdown that fluctuated between 73% and 83%, while the rest of the communes varied between 42% and 54%. Public transport decreased by 82% on average over the entire city. Regarding day-of-the-week variation, stable behavior was observed between



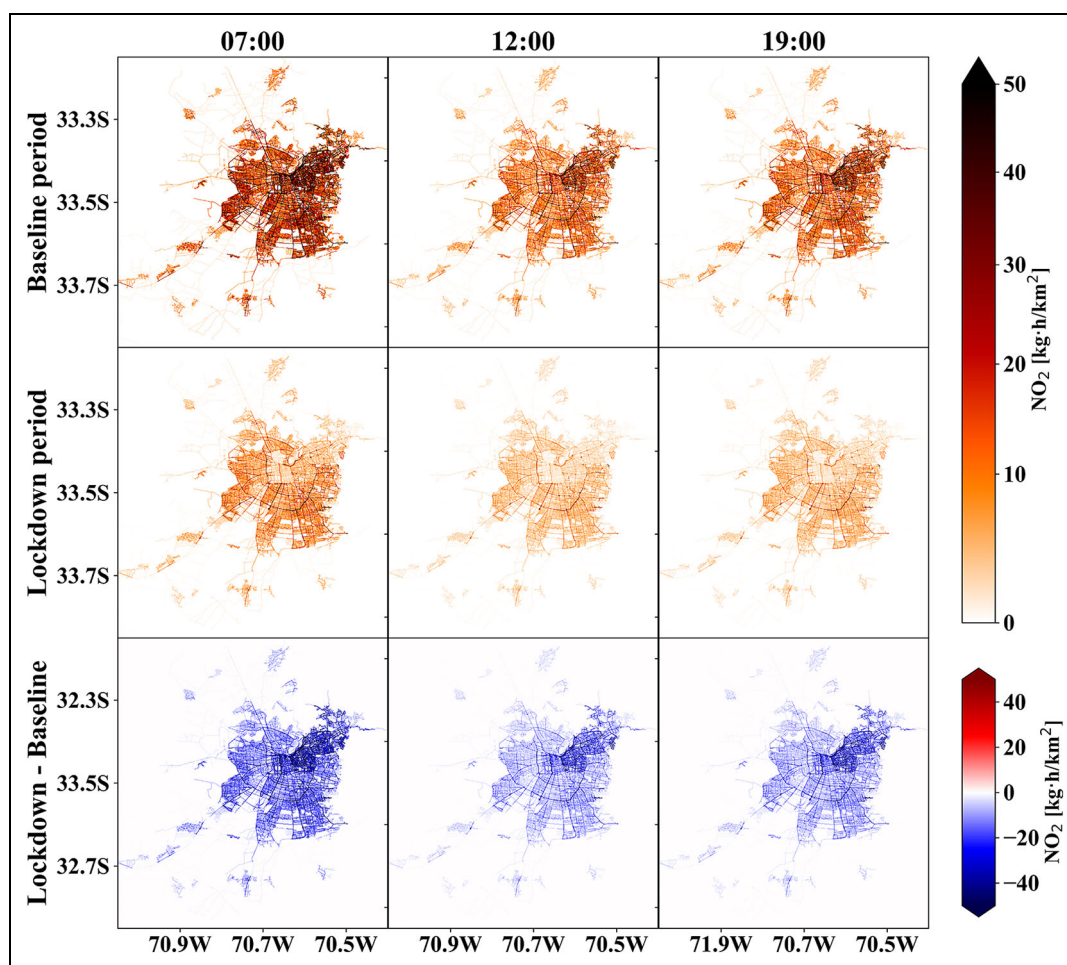


**Figure 3.**  $\text{NO}_2$  vehicle emissions in Santiago at 3 different hours. The top panels show the baseline period, the middle panels correspond to the lockdown period (March 30–April 5, 2020), and the bottom panels correspond to the difference in lockdown-baseline emissions. DOI: <https://doi.org/10.1525/elementa.2021.00044.f3>

Monday and Saturday (63%), whereas Sundays showed a slightly greater reduction (72%).

Daily VOC and  $\text{NO}_2$  emissions decreased 72% and 59%, respectively, over the entire metropolitan area of Santiago. These reductions correspond to 3.2 t/d and 7.3 t/d, respectively. The NO reduction between the baseline and lockdown conditions was 51%, corresponding to 30.4 t/d. In the communes with mandatory lockdown, VOCs and  $\text{NO}_2$  were reduced by 92%, while in the zones with voluntary restrictions, VOCs decreased by 54% (Figure S2) and  $\text{NO}_2$  by 44% (Figure 3). These results consider reduced mobility and a slight increase in average circulation speeds. The VOC/ $\text{NO}_2$  ratio in the baseline period was 0.36, which changed to 0.26 in the lockdown period. It is interesting to note that lockdown led to a significant reduction in emissions (approximately 64%) of carbon dioxide ( $\text{CO}_2$ ) from mobile sources, from 31.8 kt  $\text{CO}_2$ /d in the baseline period to 11.5 kt  $\text{CO}_2$ /d during lockdown. This highlights the importance of the transportation sector in  $\text{CO}_2$  emissions in the urban areas of Chile.

### 3.1.3. São Paulo

Analyses of traffic counts showed that during lockdown, the number of passenger cars decreased by 54%, light

commercial vehicles by 33%, light trucks by 22%, medium trucks by 16%, buses by 56%, and motorcycles by 48%, while heavy-duty trucks increased by 13%. VOC and  $\text{NO}_2$  hourly emissions and the difference between the lockdown and baseline periods (prelockdown) are shown in Figure 4. The average hourly emissions of VOCs changed from 6.5 to 3.4  $\text{kg h}^{-1} \text{km}^{-2}$ , while  $\text{NO}_2$  changed from 1.5 to 1.3  $\text{kg h}^{-1} \text{km}^{-2}$ , and the VOC/ $\text{NO}_2$  ratio changed from 9.3 to 7.7. However, these patterns varied within the larger São Paulo city, and considering the extension of São Paulo, specific local differences need to be considered. The difference between the lockdown and baseline periods for  $\text{NO}_2$  showed sharp decreases in downtown São Paulo (Figure 4).

### 3.2. Meteorology overview

The seasonal variations in rainfall, temperature, and relative humidity in 2020 and 2014–2019 for the 3 cities are presented in Figure 5. Note the sharp decrease in temperature from March to May (lockdown period) in Santiago as winter approaches, which contrasts with the constant temperatures of Bogotá, which has a more tropical climate.

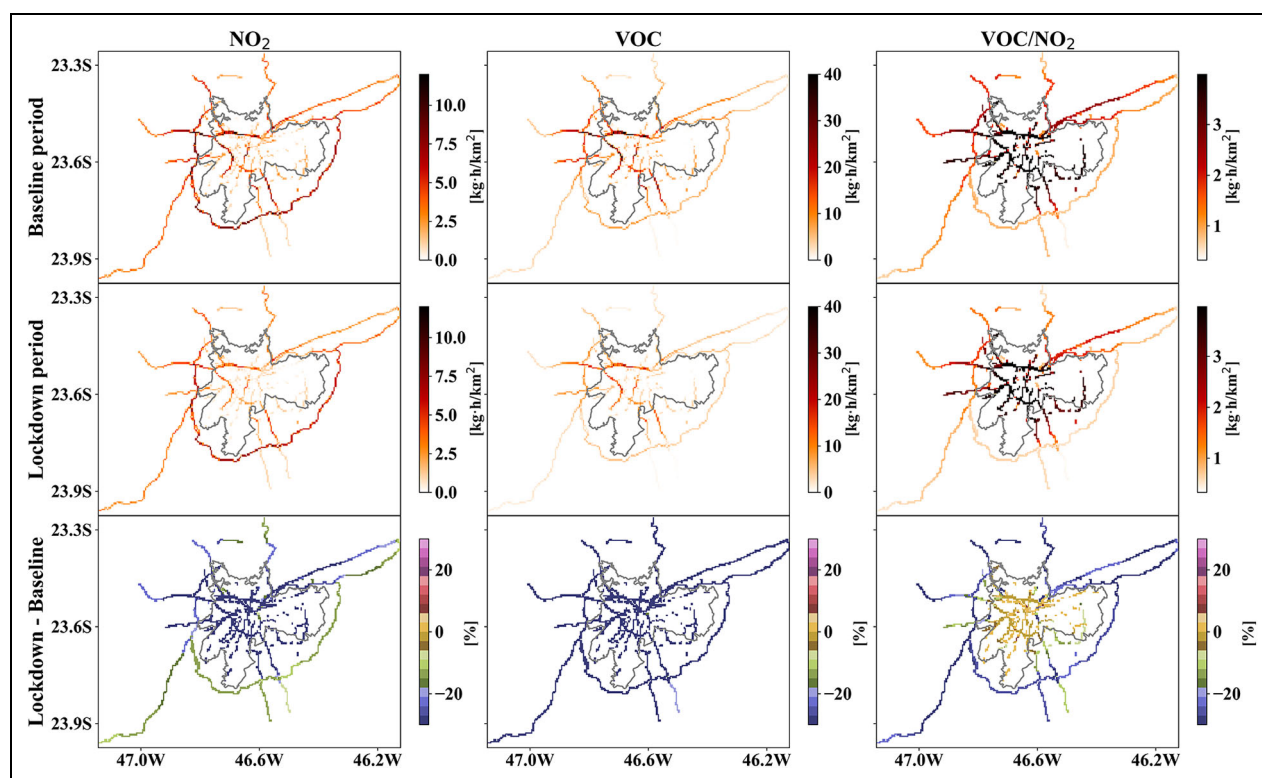


**Figure 4.**  $\text{NO}_2$  and VOC vehicle emissions and VOC to  $\text{NO}_2$  ratio determined for the baseline and lockdown period and the difference between them in São Paulo. DOI: <https://doi.org/10.1525/elementa.2021.00044.f4>

Because the prevailing meteorology can greatly influence air quality (Gkatzelis et al., 2021), 2020 was compared with 2014–2019 to identify the environmental factors that could amplify or reduce the impact of lockdowns. Typically, decreased precipitation may worsen air quality, and in terms of photochemistry, higher temperatures (lower humidity and precipitation) lead to favorable conditions for  $\text{O}_3$  formation. In the 3 cities, March–May 2020 was drier than the previous year averages (2014–2019). São Paulo was the only city to experience lower temperatures in 2020 (March–May). Temperature variations were less noticeable in Bogotá and slightly lower in Santiago. Similar findings can be found from ERA5 reanalysis-derived anomalies for March, April, and May 2020 with respect to 2015–2019 in Sokhi et al. (2021).

### 3.3. Air quality

To provide a notion of the typical values found in the central stations of Bogotá (UTC-5), Santiago (UTC-4), and São Paulo (UTC-3), **Figure 6** shows the pollution levels with diurnal cycles split into the baseline and lockdown periods. The lockdown led to significant changes in criteria air pollutants in the 3 cities (**Table 2**).

In Bogotá, the median of the daily mean concentrations of NO showed the greatest decline with respect to the baseline period (70%), followed by  $\text{PM}_{2.5}$  (40%), CO (38%), and  $\text{NO}_2$  (34%). In contrast, the median MDA8  $\text{O}_3$  mixing ratio increased (51%). The lowest increase in MDA8  $\text{O}_3$  (29%) and the lowest decrease in daily mean  $\text{PM}_{2.5}$  (18%) occurred at the Guaymaral station, located in the northern part of the city. On the other hand, the

highest increase in MDA8  $\text{O}_3$  (67%) and the greatest decrease in NO (91%) and  $\text{NO}_2$  (52%) occurred near the geographic center at the CDAR station.

In Santiago, the criteria pollutants showed a significant change during the lockdown (**Table 2**). The median for the 8 stations showed that the NO daily mean decreased the most compared with the baseline period (67%), followed by  $\text{NO}_2$  (25%), CO (20%), and  $\text{PM}_{2.5}$  (14%). The median (8 stations) MDA8  $\text{O}_3$  mixing ratios increased by 36%. The comparison of monitoring stations located in areas under lockdown (Independencia, Parque O'Higgins, and Las Condes) with those areas where other kinds of measures were implemented showed no significant differences for NO (**Table 2**). Minor differences were found for  $\text{PM}_{2.5}$  (−6%) and  $\text{O}_3$  (+7%) between stations under lockdown versus the rest of the city, while CO and  $\text{NO}_2$  showed the highest difference, both decreasing by 15% at the lockdown stations.

In São Paulo, the median of the daily mean concentrations showed the greatest reductions for the primary pollutants NO (67%) and CO (42%; **Table 2**). The median  $\text{NO}_2$  and  $\text{PM}_{2.5}$  concentrations, both of primary and secondary origin, decreased by 34% and 21%, respectively. In contrast, the median MDA8  $\text{O}_3$  concentration increased by 30%.

Overall, the ozone increases during the lockdown period negatively impacted air quality compliance. Santiago and central Bogotá recorded more days above the World Health Organization (WHO) guideline of 51 ppbv compared with the same periods of previous years (**Table 3**). This variation was much more intense in the eastern parts of Santiago, where the number of days over the



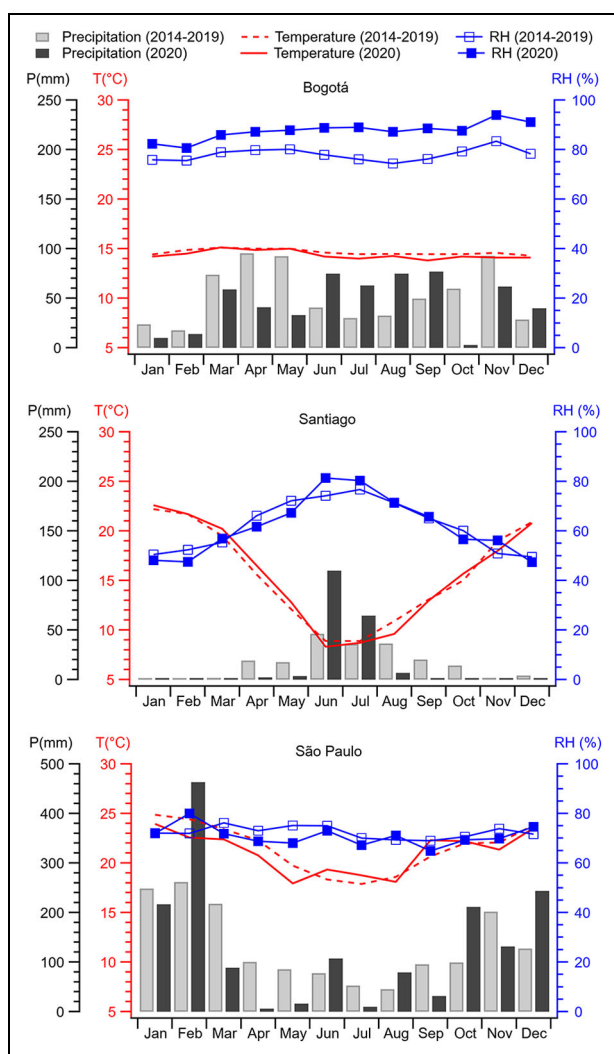


**Figure 5. Seasonal variations in precipitation (P), temperature (T), and relative humidity: a comparison between the mean values from 2014 to 2019 and 2020.** Bogotá: Airport Station (4.712518,  $-74.149141$ ), central Santiago: Quinta Normal Station ( $-33.44500$ ,  $-70.67778$ ), and central São Paulo: Pinheiros Station (precipitation obtained from the Institute of Astronomy, Geophysics, and Atmospheric Sciences–Universidade de São Paulo Weather Station:  $-23.65$ ,  $-46.62$ ). DOI: <https://doi.org/10.1525/elementa.2021.00044.f5>

guideline rose to 18 days. In São Paulo, some central stations retained similar exceedances or slightly increased, as seen at Park IBI SP, where the number of  $O_3$  exceedances reached 16 days. It is worth mentioning that WHO guidelines allow 4 days above 51 ppbv per year (99th percentile of the MDA8  $O_3$ ).

### 3.4. $NO_2$ tropospheric columns

Despite cloudiness, the reduction in  $NO_2$  columns can be seen over and downwind of the 3 cities in the TROPOMI  $NO_2$ , showing parallels with the estimated reductions in mobile emissions (Figure 7). The median declines in  $NO_2$  columns over Bogotá, Santiago, and São Paulo during lockdown were 40%, 35%, and 47%, respectively (Table S3). By

relaxing cloud filtering over Bogotá and São Paulo, we estimated the decline in the  $NO_2$  column 15-day periods, as shown in Table S3. In this manner, we found that while Bogotá and Santiago showed the largest decreases in the second half of March, 70% and 44%, respectively, São Paulo achieved the largest reduction (66%) in the first half of May. The decrease in Bogotá coincided with the largest reduction in mobility, as shown in Figure 1. In Santiago, the maximum  $NO_2$  column reduction coincided with the quarantine over the 7 wealthiest districts and nighttime curfew elsewhere in the metropolitan area, which led to an overall mobility reduction of ca. 50%–60% according to Google data. In late May, mobility in Santiago reached its lowest values, coinciding with a national holiday and with the progressive extension of the lockdown over the whole metropolitan area; however, this was not reflected in the  $NO_2$  column due to increased cloudiness that interfered with the satellite retrieval. Additionally, May was typically cold, and thus, residential emissions increased. In São Paulo, mobility was most reduced (50%–60%) in late March and April 1–15, which coincided with a 56% reduction in the  $NO_2$  column. In the first half of May, when the decrease in the  $NO_2$  column was strongest (66%), mobility increased, suggesting there was a decrease in sources other than vehicles.

### 3.5. Photochemical changes

The substantial reduction in VOC and  $NO_x$  emissions resulted in a photochemical regime shift. The ambient  $NO_2$  to  $NO_x$  ratio was higher during the lockdown period than during the baseline period in Bogotá, Santiago, and São Paulo (Figure 8). In these 3 cities, less NO was available to titrate  $O_3$  due to fewer vehicle emissions, and the conversion of NO to  $NO_2$  was favored. As a result of these 2 chemical processes,  $O_3$  increased at all stations studied in Bogotá, Santiago, and São Paulo (Figure 8). Furthermore, CO, which can be used as a proxy for VOCs, was useful for inferring that the VOC to  $NO_x$  ratio increased in the lockdown period. In Santiago, for example, higher MDA8  $O_3$  was reached on days when CO was similar to the baseline period mean (Figure 8).

In Santiago, during the lockdown period, the  $O_3$  mixing ratio was also modulated by the temperature, reaching the highest MDA8 values on days with higher daily mean temperature and the lowest MDA8 on cloudy or rainy days (Figure 8). This correlation was particularly relevant for central Chile, where increasing heat waves were leading to more  $O_3$  exceedances (Seguel et al., 2020) and wildfires (Jacques-Coper et al., 2021).

It is also worth noting that from January to April 2020, fire activity in Colombia and Venezuela was much more intense than the 2014–2019 average, peaking in February and March in Colombia and as late as April in Venezuela (Mendez-Espinosa et al., 2020). The impact of biomass-burning events continued during the lockdown period but was less severe than before.

### 3.6. Photochemically driven changes in aerosols and AOD

We estimated the secondary fractions of aerosols at representative sites in Bogotá, Santiago, and São Paulo for the

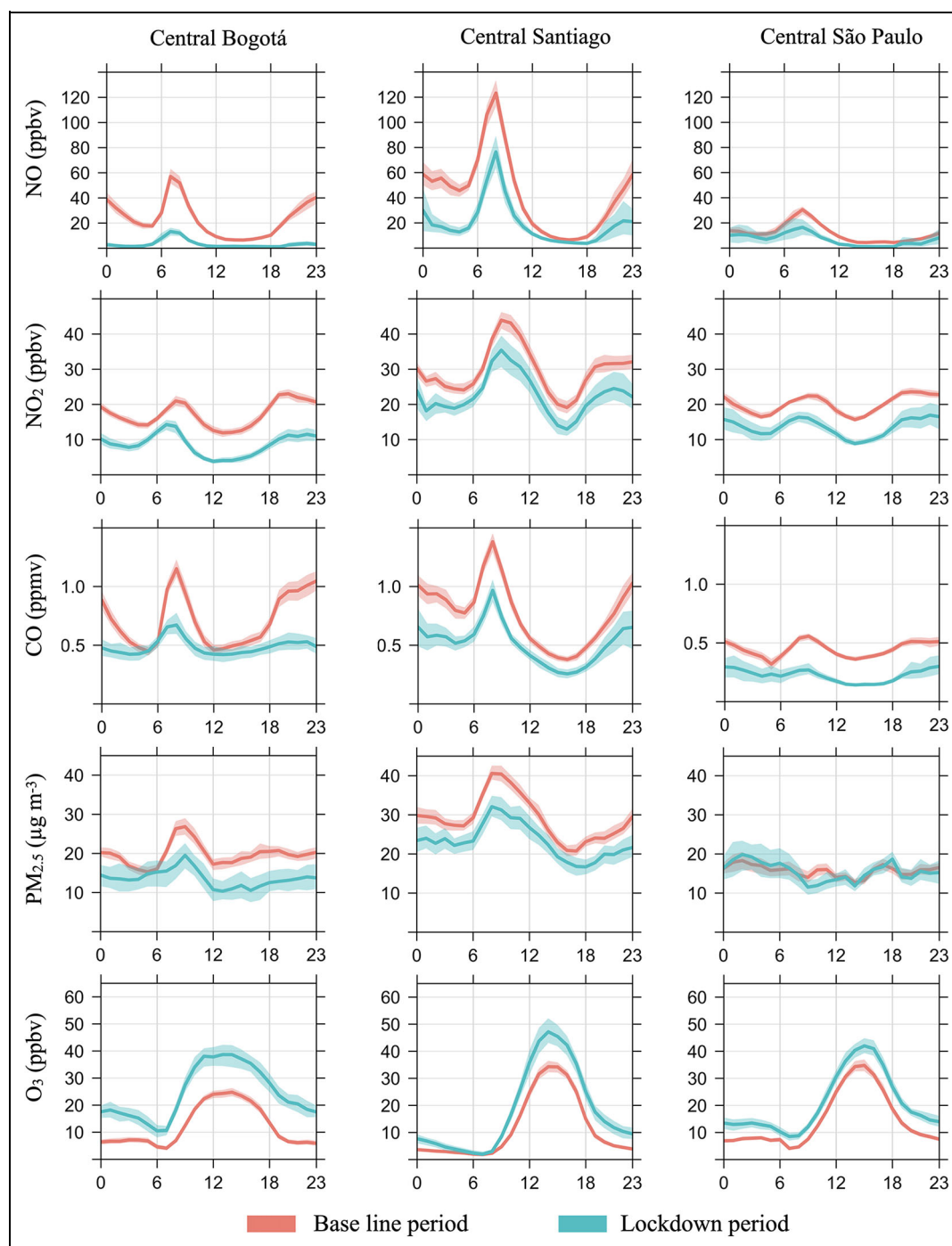


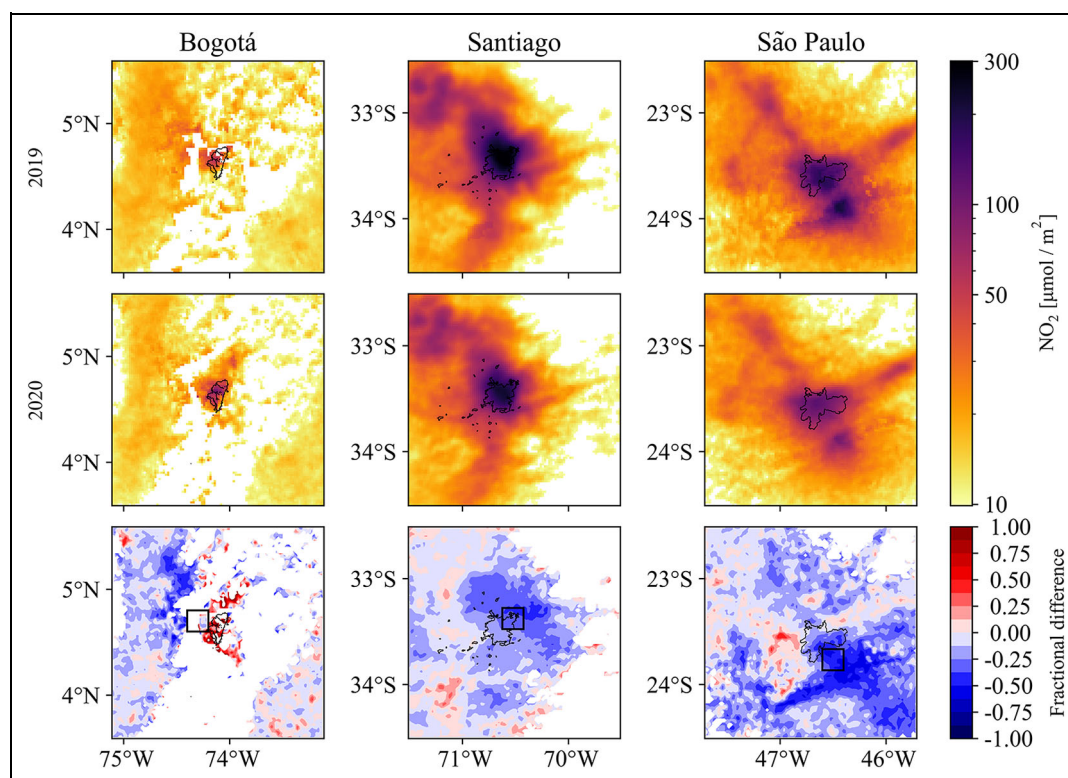
**Figure 6. Central Bogotá (CDAR), central Santiago (Parque O'Higgins), and central São Paulo (Parque Dom Pedro) average diurnal cycles of NO, NO<sub>2</sub>, CO, PM<sub>2.5</sub>, and O<sub>3</sub> split into the baseline and lockdown periods.** The shading shows the 95% confidence intervals of the mean. DOI: <https://doi.org/10.1525/elementa.2021.00044.f6>

base and lockdown periods, as illustrated in Figure S3. The largest fraction of secondary aerosols was found in eastern Santiago, where secondary aerosols made up 55% and 61% of the daily average concentrations of PM<sub>2.5</sub> under the base (approximately 21  $\mu\text{g m}^{-3}$ ) and lockdown (approximately 16  $\mu\text{g m}^{-3}$ ) scenarios, respectively. Southwestern Bogotá had the highest daily averages of PM<sub>2.5</sub> and the lowest fractions of secondary aerosols during the baseline (35% of 34  $\mu\text{g m}^{-3}$ ) and lockdown periods (37% of 25  $\mu\text{g m}^{-3}$ ). At all sites, either no changes or slight increases in the secondary aerosol fraction was found,

from zero percentage points (pp) at Pinheiros in São Paulo to 6 pp in eastern Santiago. In all sites studied, increased O<sub>3</sub> mixing ratios were observed over a broad range (6 pp at São Paulo and 69 pp at central Bogotá during lockdown), which suggests an intensification of photochemical activity consistent with the VOC-limited regimes identified earlier, as well as secondary aerosol formation. However, this growth was counteracted by the decrease in primary emissions that resulted in lower concentrations of daily average PM<sub>2.5</sub>, NO, and NO<sub>2</sub>. The only sites where we inferred an increase in the absolute concentrations of

**Table 3.** Number of World Health Organization guideline exceedances in monitoring station of Bogotá, Santiago, and São Paulo. DOI: <https://doi.org/10.1525/elementa.2021.00044.t3>

City	Station Name	2014	2015	2016	2017	2018	2019	2020
Bogotá	1. Carvajal–Sevillana	0	0	–	0	0	0	0
	2. Centro de Alto Rendimiento–CDAR	2	1	–	–	–	0	13
	3. Guaymaral	3	0	1	0	0	1	0
	4. Tunal	0	0	–	0	0	0	0
Santiago	1. Cerro Navia	0	0	–	0	1	4	4
	2. El Bosque	0	1	0	0	0	3	1
	3. Independencia	–	0	0	0	1	3	3
	4. La Florida	0	0	0	0	1	–	–
	5. Las Condes	1	10	0	1	1	5	18
	6. Parque O'Higgins	–	3	0	1	7	3	10
	7. Pudahuel	0	0	0	0	0	4	4
	8. Puente alto	0	2	1	1	7	7	11
São Paulo	2. Ibirapuera (Park IBI SP)	6	7	14	2	8	12	16
	4. Parque Dom Pedro (Central DP SP)	1	3	7	1	4	5	5
	5. Pinheiros (Central PIN SP)	1	2	9	0	0	4	2

**Figure 7.** TROPospheric Monitoring Instrument (TROPOMI)/Sentinel5P NO<sub>2</sub> tropospheric column in  $\mu\text{mol}/\text{m}^2$  averaged for the reference period in 2019 (upper panel) and corresponding columns for the lockdown period in 2020 (middle panel). The lower panel shows the fractional difference NO<sub>2</sub> columns (i.e., 2020 minus 2019 over 2019 values). Data can be retrieved from the released offline version of the TROPOMI tropospheric NO<sub>2</sub> columns at <https://s5phub.copernicus.eu>; <http://www.tropomi.eu>. DOI: <https://doi.org/10.1525/elementa.2021.00044.f7>



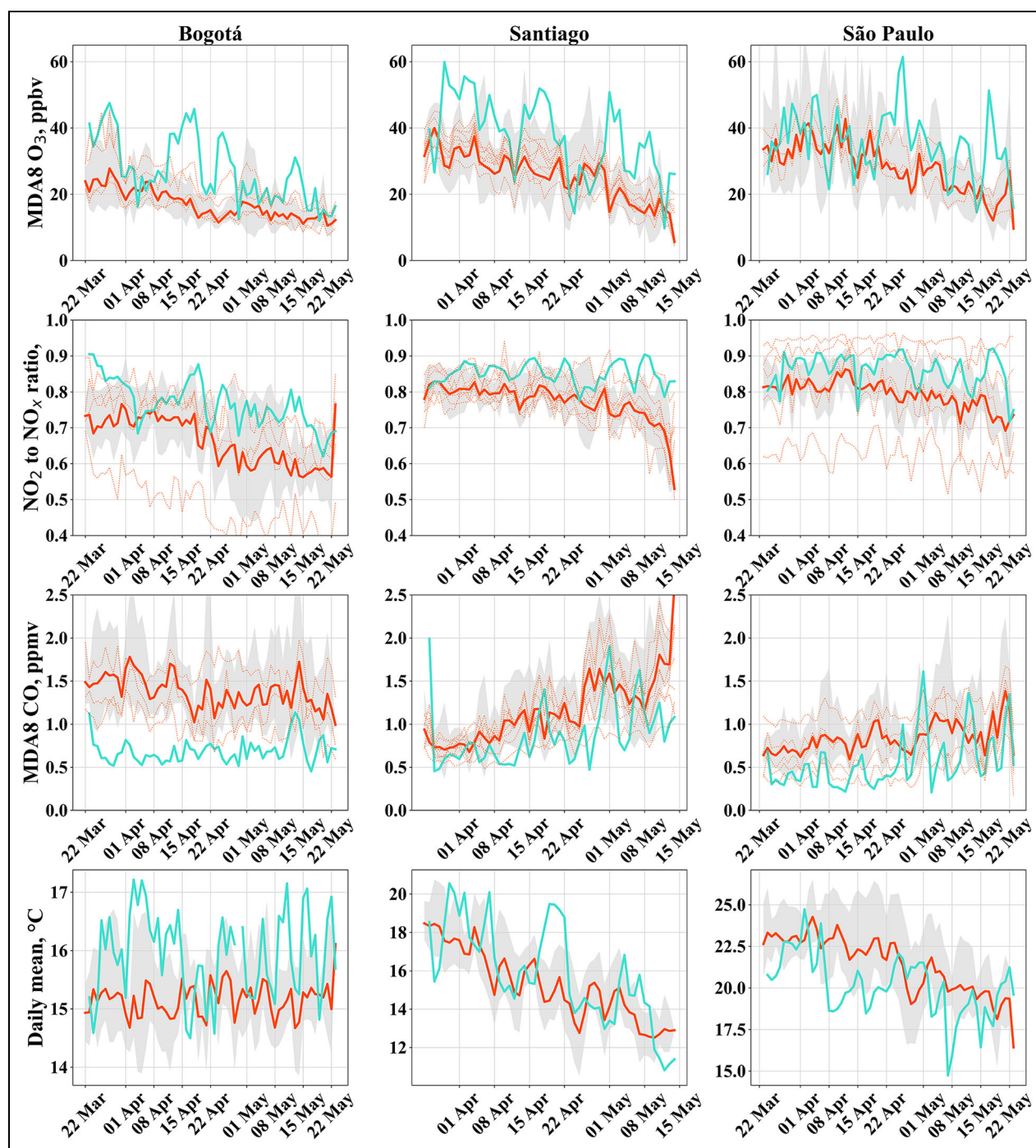


**Figure 8.** Maximum daily 8-h average (MDA8) of O<sub>3</sub>, NO<sub>2</sub> to NO<sub>x</sub> ratio (determined from MDA8 metrics), MDA8 of CO and temperature daily mean for Bogotá (left panel), Santiago (middle panel), and central São Paulo (right panel). The red line represents the mean of all stations for the 2014–2019 period. The shading shows the 95% confidence intervals of the mean. The red dotted line shows every single year between 2014 and 2019. The green solid line represents all stations for the lockdown period. DOI: <https://doi.org/10.1525/elementa.2021.00044.f8>

secondary aerosols were in western and central Santiago (approximately 8 pp); thus, at these sites, secondary aerosol production must have surpassed the effect of lower primary emissions.

Concerning changes in AOD, in Santiago, the AOD daylight cycle had a small shift in the maximum from 11:00 to 12:00 (local time). Additionally, a second maximum developed at 17:00 (Figure S4). Before the noon

maximum, the lockdown average had a reduction in AOD with respect to the baseline period, while for the secondary maximum, a slightly larger value of AOD during 2020 was found than in previous years at the same hour. Regarding the AE, daylight cycles showed a similar shape to previous years, except for a notable reduction in the value of the AE for all spectral ranges considered (Figure S5 shows one such spectral range), with values lower than

**Table 4.** Generalized additive model error statistics at Gauymaral in Bogotá, Las Condes in Santiago, and Ibirapuera in São Paulo for the base period (2015–2019) and the lockdown period. DOI: <https://doi.org/10.1525/elementa.2021.00044.t4>

City	Especies	2015–2019				Lockdown			
		R	RMS (ppbv)	MAPE (%)	N	R	RMS (ppbv)	MAPE (%)	N
Bogotá	MDA8 O <sub>3</sub>	.8	6.0	15	284	.7	13.0	24	51
Santiago		.9	7.4	21	235	.7	17.5	34	57
São Paulo		.8	9.0	14	300	.7	10.4	22	60
Bogotá	MDA8 NO <sub>2</sub>	.6	7	18	221	.5	10.0	81	59
Santiago		.6	11.2	14	250	.7	22.6	98	57
São Paulo		.7	6.7	16	282	.7	9.2	68	57

The statistics are Pearson correlation (R), root mean square (RMS), and mean absolute percentage error (MAPE). Also, the number (N) of data points is indicated.

1 standard deviation from the distribution of previous years.

In São Paulo, the daylight cycle of AOD and AE between 9:00 and 17:00 (local time) showed a decrease during the lockdown period compared with the baseline period (Figure S4). However, the maximum at 15:00 remained during the lockdown period and then remained relatively high. As in Santiago, changes in AOD remained within the variability of previous years, with a less substantial reduction in the AE than in Santiago, with values within the variability of previous years.

The AOD depends not only on the total aerosol burden but also on the size distribution. In general, small particles scatter light more efficiently than large particles; if 2 air masses contain the same aerosol burden, a larger AOD will result from the air mass with the larger concentration of smaller particles (e.g., Schuster et al., 2006, Huneus et al., 2011). Therefore, changes in the combined AOD and AE can suggest relative changes in the size distribution. Based on this, the reduction in the AE could be produced either by a decrease in fine mode particles or an increase in the coarse mode fraction. The reduction in the AE with a decrease in AOD suggests a decrease in the fine mode particles, consistent with emission decreases caused by the significant decrease in mobile sources during the lockdown period. However, comparable AE and AOD values and even larger AOD values suggest an increase in the coarse mode fraction. The latter could be a result of the arrival of aged air parcels, intrusion of coastal air with marine aerosols, resuspension of dust particles, and/or a combination of these.

### 3.7. Role of meteorology and other factors

In the reference periods, the GAMs showed good error statistics for all cities (Table 4), with Pearson correlations for O<sub>3</sub> (NO<sub>2</sub>) of approximately or above 80% (60%) and root mean square errors below 9 (11) ppbv for O<sub>3</sub> (NO<sub>2</sub>). These error statistics were worse during the lockdown period, which was expected since there were fewer data and because the GAM estimates did not account for

changes due to lockdown, that is, vehicular circulation or activity patterns.

Regarding the physical interpretation of the O<sub>3</sub> GAM, we found a linear positive dependence on daily maximum temperatures for Santiago and São Paulo, whereas in Bogotá, it was slightly nonlinear (Figure 9). These results are based on in situ measurements and consistent with other descriptions found in the literature (e.g., Porter and Heald, 2019). Positive linear dependences on solar radiation were found in Santiago and São Paulo, whereas over Bogotá, the relationship was linear. The former is consistent with intensified photochemical activity triggered by radiation. The weak dependence of ozone on solar radiation in Bogotá is somewhat surprising to us, and we hypothesize that this weak dependence results from the competition between increased solar radiation (closer to the equator) and the relatively high abundance of ultraviolet radiation due to its high altitude, leading to O<sub>3</sub> photolysis.

Only in São Paulo, there was an inverse relationship between O<sub>3</sub> and specific humidity (and relative humidity), as documented in other studies (e.g., Camalier et al., 2007). In Bogotá and Santiago, the relationship was slightly nonlinear but positive. The reasons for the different dependences in these 3 cities are unclear and require further investigation, including the role of deposition processes (e.g., Kavassalis and Murphy, 2017). The dependence on the maximum wind speed was quite different among the selected stations. In the case of Bogotá and Santiago, the stations considered were receptor sites. In Bogotá, the relationship was weak but positive (mostly during calm conditions). In Santiago, the relationship was nonlinear, with a positive dependence under nearly calm conditions (as in Bogotá) and an inverse relationship above 2 m/s, indicating the effect of dilution. In São Paulo, the relationship was clearly inversed, also suggesting dilution for winds below 3 m/s. With respect to the day of the week, Santiago had a clear weekend effect. In São Paulo, O<sub>3</sub> mixing ratios also steadily increased over the week from Monday to Sunday. Bogotá had no variations over the week for O<sub>3</sub>. However, the weekend effect was clearer as



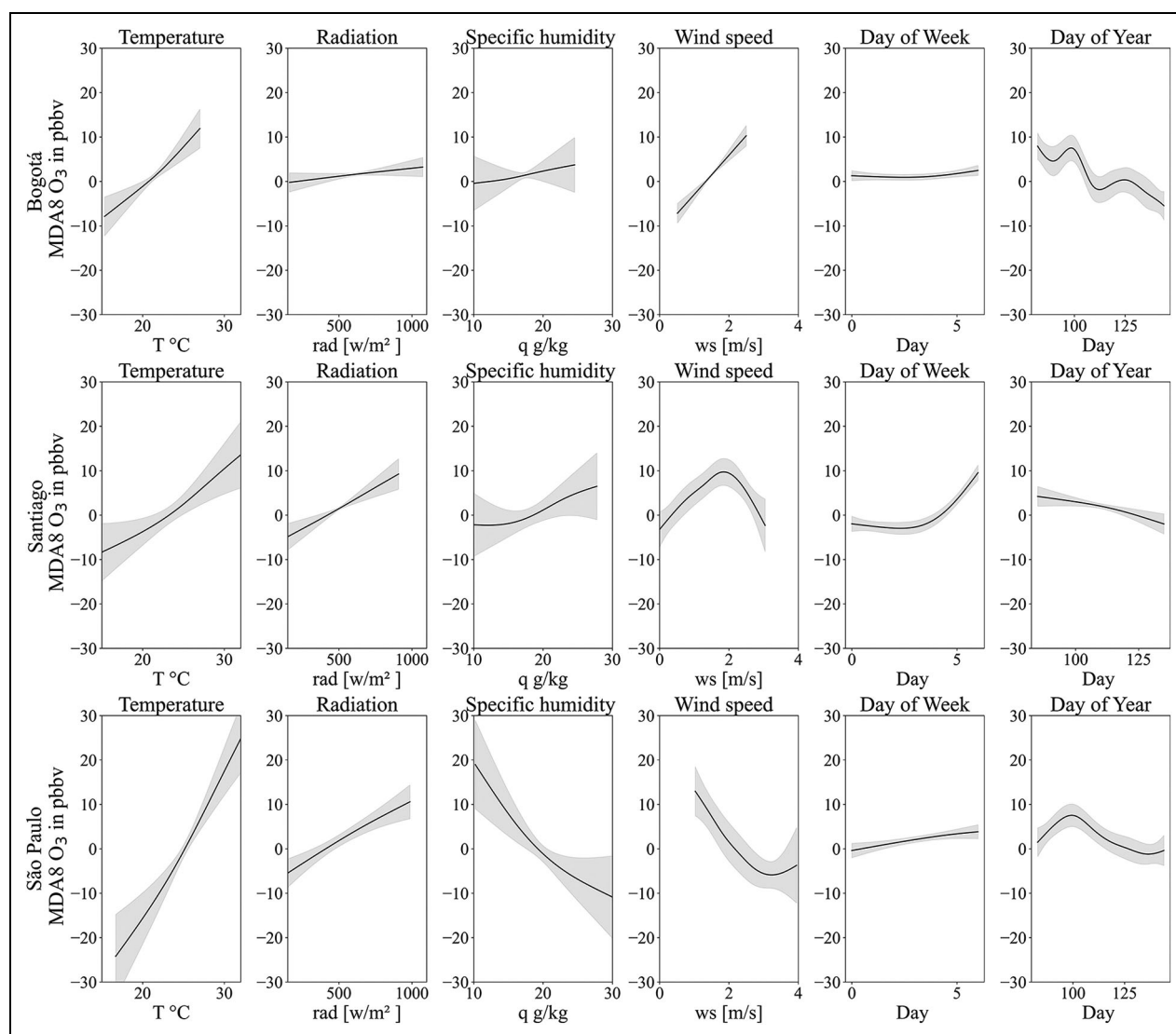


**Figure 9.** Partial dependence plots for  $O_3$  in the generalized additive model for Bogotá, Santiago, and São Paulo. Variables are daily maximum temperature ( $T$ ), solar radiation ( $rad$ ), specific humidity ( $q$ ), wind speed ( $ws$ ), day of the week, and Julian day ( $JD$ ). DOI: <https://doi.org/10.1525/elementa.2021.00044.f9>

$NO_2$  declined (Figure S7). Finally, regarding seasonality (Julian day) dependence, we found a progressive decline in  $O_3$  as the cold season approached in Santiago. On the other hand, in Bogotá, the impact of savannah fires early in the year was clear and led to a progressive  $O_3$  decline, with a small break in the trend in early May ( $JD \approx 125$ ). São Paulo had an increase in  $O_3$  in early March ( $JD \approx 100$ ). Hence, the partial dependences of the  $O_3$  GAM appeared to be physically justified. Something similar occurred in the case of the  $NO_2$  GAM (see Supplementary Material, Figure S7).

In all 3 cities, the GAM outputs (Figure 10) indicate that observed increases in  $O_3$ —with respect to GAM-adjusted values—were often attributable to factors other than local meteorology and typical—as captured by the 2015–2019 variability—weekly and seasonal changes. During the lockdown, the GAM results indicate median increases in MDA8  $O_3$  of 9 ppbv (26%), 15 ppbv (35%), and 8 ppbv (19%) in Bogotá, Santiago, and São Paulo, respectively, when compared with the corresponding

multiyear baseline period. However, over the approximately 1-month-long lockdown periods, there was also a significant portion of days when meteorological, weekly, and seasonal changes explain the observed variability.

In São Paulo, the  $O_3$  GAM captured most of the variability found in the observations. This indicates that changes in mobility, precursor emissions, and ozone were relatively minor. Only a few days in the second half of April showed a distinct behavior, with increased ozone values. Overall, these features are consistent with less stringent mobility reductions and the modest decreases in  $NO_2$  values, as shown in Figure S8, as well as in estimated  $NO_x$  emissions from mobile sources. This may be explained by the fact that lockdown was applied only to downtown areas of the vast metropolitan area of São Paulo. Interestingly, the Easter weekend resulted in a minor  $O_3$  increase due to less mobility. Something similar occurred in Bogotá and Santiago, except that in Santiago, a sharp  $O_3$  decrease was seen in connection with cloudy conditions and light precipitation in Santiago (not shown).

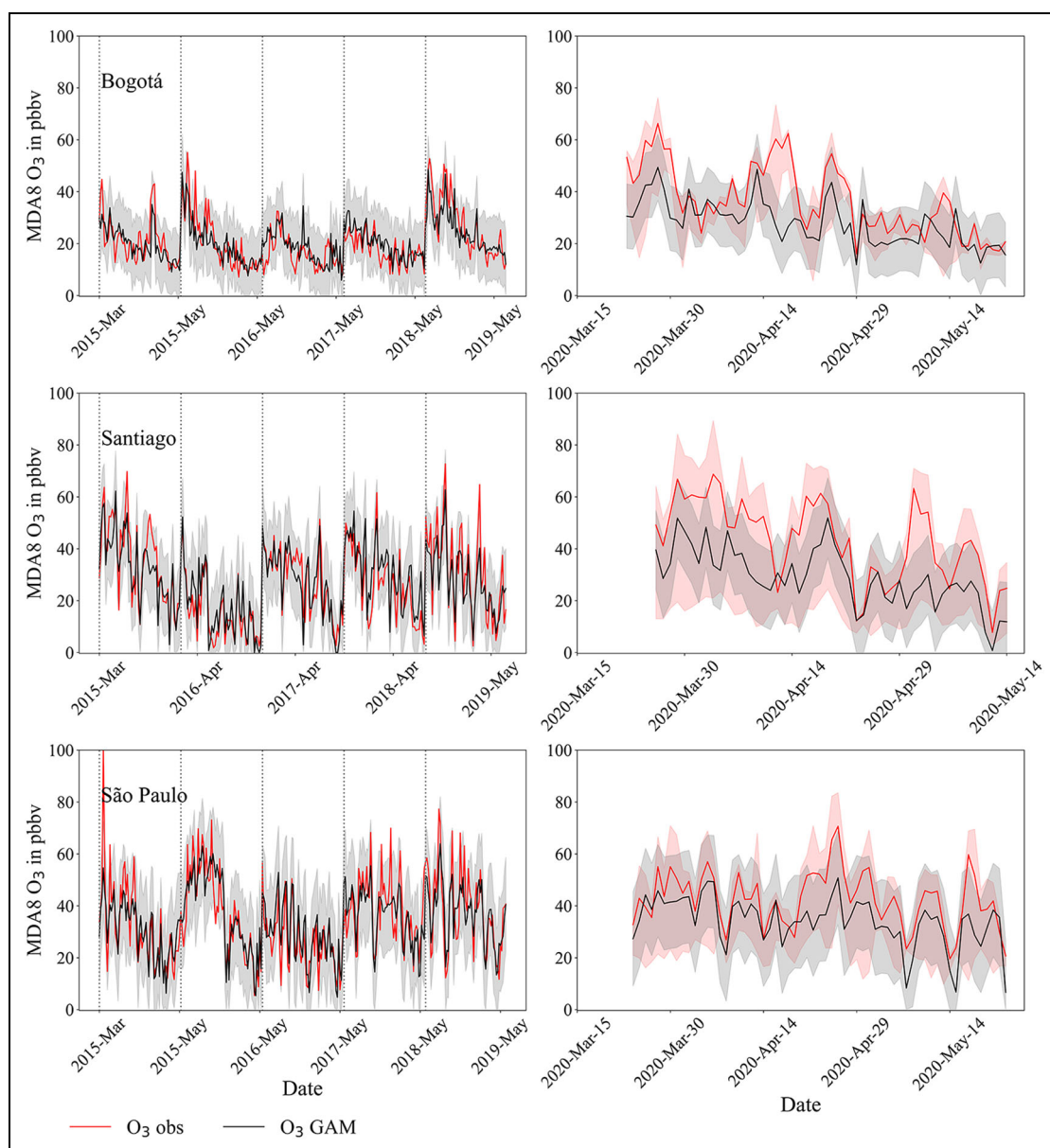


**Figure 10.** Observed (red line) and generalized additive model (GAM-fitted (black line) maximum daily 8-h average O<sub>3</sub> for Bogotá (upper panels), Santiago (middle panels), and São Paulo (lower panels) for the base period (2015–2019) in the left panels and the lockdown in 2020 in the right panels. In the left panels, the vertical gray lines indicate the period of the year considered, that is, only March to May of each year. In the right panels, the gray shading corresponds to the confidence interval of the GAM, and the reddish shading corresponds to the variation in the observations (percentiles 0.01 and 0.99). DOI: <https://doi.org/10.1525/elementa.2021.00044.f10>

In Bogotá, one can distinguish 3 periods with O<sub>3</sub> increases with respect to the GAM-adjusted values. However, only the first episode of O<sub>3</sub> increase in late March was readily attributable to NO<sub>x</sub> decreases. The remaining O<sub>3</sub> episodes did not show strong decreases in NO<sub>2</sub> as estimated by the GAM method. Thus, we hypothesize that in addition to the reduction in NO<sub>x</sub> emissions, the increase in O<sub>3</sub> may have been due to long-range transport of O<sub>3</sub> from areas upwind of Bogotá.

The strongest simultaneous NO<sub>2</sub> decrease and O<sub>3</sub> increase occurred in Santiago, concurrently with the lockdown enforced over the wealthiest areas (March 23–April 10), highlighting the disproportionate role played by these

communes in driving Santiago's mobility. A secondary O<sub>3</sub> increase episode occurred around May 22, which also coincided with a decrease in GAM-adjusted NO<sub>2</sub>. The third largest O<sub>3</sub> increase occurred on approximately May 11, that is, the International Labor Day, when decreased mobility was still accompanied by clear skies providing appropriate conditions for photochemistry. We also found more modest O<sub>3</sub> increases and NO<sub>2</sub> decreases on approximately May 11 in Bogotá and São Paulo.

### 3.8. Uncertainties in data and methods

Emissions were calculated using a bottom-up methodology (Tolvett Caro et al., 2016). This approach considered

**Table 5.** Percentage declines in median NO<sub>2</sub> values from the reference period (2015–2019) and the lockdown in NO<sub>2</sub> derived from generalized additive model (GAM) calculations at Guaymaral in Bogotá, Las Condes in Santiago, and Ibirapuera in São Paulo; TROPospheric Monitoring Instrument (TROPOMI) NO<sub>2</sub> column over the urban areas; in situ NO<sub>2</sub> observations, and emission estimates. DOI: <https://doi.org/10.1525/elementa.2021.00044.t5>

City	GAM	TROPOMI	In Situ Observations	Emissions
Bogotá	31 (–1 to 59)	40 (2 to 70)	33 (0 to 53)	30 to 71 NO <sub>x</sub>
Santiago	50 (14 to 69)	35 (18 to 44)	44 (16 to 61)	44 to 92 NO <sub>2</sub>
São Paulo	34 (–2 to 68)	47 (–7 to 66)	34 (–3 to 65)	24 NO <sub>2</sub>

Corresponding ranges are also shown. A negative number indicates increases.

vehicle activity from several sources, as presented in Table S1. While both the approach and the data contain measurement errors and uncertainties, we deem the quality and consistency sufficient to assess the changes in emissions that occurred in connection with mobility restrictions in early 2020.

Instruments and methods used for measuring pollutants in governmental agencies follow international standards and are subject to quality assurance and control, which provides a robust dataset in all cities. Nevertheless, the data used in our study were subject to further quality checking by the authors; thus, we ascertained that we used a reliable dataset of comparable quality to those considered in other studies performed elsewhere in the world and in the region. The characteristics of each measurement station correspond to location, and their representativity may vary according to the pollutant, time of the year, and so on (e.g., Osses et al., 2013). These factors may result in uncertainties in estimating the air quality changes in cities that are heterogeneous.

The lack of time- and space-resolved VOC measurements in ambient air is an important limitation for characterizing the photochemical regimes in all 3 cities. However, the high agreement between the different observation techniques described in this article points toward the validity of our findings.

The consistency in observations is shown in **Table 5**, using NO<sub>2</sub> as an example. Both in situ and remote sensing methodologies indicated consistent fractional declines in NO<sub>2</sub>. However, as these methodologies are different, they are not quantitatively comparable, but both show consistency regarding the changes observed.

In this study, we limited the length of lockdown to the active photochemical period. In these periods, we did not quantitatively examine the relationships between lockdown measures and public adherence.

The GAM calculations applied a Bayesian approach (Wood, 2017), where a covariance matrix was calculated to find the confidence intervals of the model estimate. Thus, the shaded area in **Figure 10** corresponds to the confidence intervals between the 0.25 and 0.75 quantiles.

#### 4. Conclusions

In Bogotá, Santiago, and São Paulo, the improvement in air quality due to emission reductions of primary pollutants at the start of the 2020 pandemic was lessened to

some extent by the formation of secondary pollution, particularly in Santiago. Thus, air quality improved in terms of ground-level PM<sub>2.5</sub> at all stations, especially in industrialized areas of Bogotá. However, O<sub>3</sub> and secondary pollution worsened, mainly but not solely at the receptor sites in Bogotá, Santiago, and São Paulo.

The change in NO<sub>2</sub> vehicle emissions was nearly proportional to the in situ measurement of NO<sub>2</sub> mixing ratios and satellite-based tropospheric columns in Santiago and São Paulo, thus showing its direct impact on air quality and the importance of vehicle emissions in these cities. In all 3 cities, urban inequity results in differentiated emission patterns and pollution burdens, especially in Santiago, where the mobility of the wealthiest areas considerably impacts the rest of the city.

The vehicle emission rates of VOCs and NO<sub>x</sub> calculated using available inventories for Bogotá, Santiago, and São Paulo revealed the different technological stages that these cities currently have for abating these pollutants.

The AOD decreased in the central locations of Santiago and São Paulo during the early lockdown. The AE indicated that slight reductions in particle size occurred during daylight hours in São Paulo and in the mornings in Santiago. The slight increase in the AE during the afternoon hours in Santiago, on the other hand, suggests an increase in coarser particles.

During lockdown periods, the O<sub>3</sub> sensitivity to daily maximum temperatures provides evidence of the expected air quality changes under a scenario of NO<sub>x</sub> emission reduction, highlighting photochemistry's key role in these cities. This relationship is key in estimating the O<sub>3</sub> climate penalty; however, it must be further investigated in line with other meteorological variables. Nevertheless, these sensitivities must be considered when developing air quality and climate mitigation strategies.

Because of the lack of time- and space-resolved VOC measurements in these megacities, the quantitative role of VOCs in O<sub>3</sub> formation and source attribution could not be addressed. However, the significant and consistent O<sub>3</sub> increases suggest that reactive VOC sources other than fossil fuel-powered vehicles played a key role in the photochemical production of NO<sub>2</sub> and subsequent formation of O<sub>3</sub> during the lockdown in these megacities.

Even though all cities showed substantial declines in mobility and vehicle emissions, particularly during the early lockdown, only Santiago exhibited sustained

increases in oxidants ( $O_x = O_3 + NO_2$ ) and secondary aerosols. In the case of São Paulo, the lack of observed sensitivity may be explained, in part, by less adherence over the whole and extended metropolitan area, which mitigated the changes that were only strictly enforced downtown. In Bogotá, despite large mobility and emission declines, the increase in oxidants was possibly mitigated by intense radiation. Hence, all cities are photochemically sensitive to changes in emissions, but this sensitivity is strongly modulated by local meteorology. In Bogotá, high altitude and intense ultraviolet radiation can have significant effects on driving photochemistry.

The GAM methodology provided further insights into the physical explanation of the observed changes. Interestingly, all cities showed a strong dependence on local meteorology once seasonality and weekly urban activity patterns were accounted for. This opens opportunities for forecasting secondary pollution and for addressing climate penalties. Beyond this statistical analysis, physical models and more detailed emission estimates are required to better understand the underlying physical and chemical processes and to better define mitigation options. This study presents the differing sensitivities in Bogotá, Santiago, and São Paulo to substantial but unevenly distributed mobility changes.

Finally, this unintended experiment highlighted that mobility plays a key role in all cities and the pivotal role of photochemical processes. However, their intertwined nature stresses that environmental policies must consider not only technological solutions but also behavioral changes and social, economic, and environmental inequity in our cities.

#### Data accessibility statement

All data used in this article are publicly available in the repositories indicated in the methodology or supplemental material. Surface data of Bogotá, Santiago, and São Paulo were compiled at Pangaea (<https://doi.pangaea.de/10.1594/PANGAEA.940302>). Data on mobile source emissions for São Paulo can be found at [https://github.com/atmoschem/vein/tree/master/projects/MASP\\_2020](https://github.com/atmoschem/vein/tree/master/projects/MASP_2020) and for Santiago and Bogotá at <https://data.mendeley.com/datasets/y8drryy2yc/1>.

#### Supplemental files

The supplemental files for this article can be found as follows:

Figures S1–S8. Tables S1–S3. Docx

#### Acknowledgments

Traffic data for Santiago, March–April 2020, were kindly provided by Unidad Operativa de Control de Tránsito. We are grateful to the CETESB ([www.cetesb.sp.gov.br](http://www.cetesb.sp.gov.br)) in São Paulo for providing access to air pollutant data. The open-source R programming language, the integrated development environment RStudio (<https://www.r-project.org>), and its package Openair (<http://www.openair-project.org>) were used for statistical computing and plotting pollutant hourly data. We thank Axel Osses for advising on the applicability of the generalized additive model method to model time series.

#### Funding

This work was supported by ANID/FONDAP/15110009; Prediction of Air Pollution in Latin America and the Caribbean project (ID: 777544, H2020-EU.1.3.3). MFA, EL, and TN acknowledge FAPESP (project 2016/18438-0). NH was also supported by the Research and Innovation programs under grant agreement 870301 (AQ-WATCH) and by the MAP-AQ, which is an International Global Atmospheric Chemistry (IGAC)- and World Meteorological Organization (WMO)-sponsored activity. MO acknowledges support from ANID PIA/APOYO AFB180002.

#### Competing interests

The authors declare no competing interests.

#### Author contributions

- Contributed to conception and design: RS, LG, MO, NR, TN.
- Contributed to the acquisition of data: RS, LG, MO, NR, TN, CM, PC, HE, SI, EL, ML, SM, FM, GM, NP, SP, JR, RR, ISA, RT, AY.
- Contributed to the analysis and interpretation of data: RS, LG, MO, NR, TN, CM, LB, NH, SI, EL, SM, NP, SP, RR.
- Drafted and/or revised this article: RS, LG, MO, NR, TN, CM, MFA, ZF, SM.

#### References

- Andreae, MO, Crutzen, PJ.** 1997. Atmospheric aerosols: Biogeochemical sources and role in atmospheric chemistry. *Science* **276**(5315). DOI: <http://dx.doi.org/10.1126/science.276.5315.1052>.
- Barraza, F, Lambert, F, Jorquera, H, Villalobos, AM, Gallardo, L.** 2017. Temporal evolution of main ambient PM<sub>2.5</sub> sources in Santiago, Chile, from 1998 to 2012. *Atmospheric Chemistry and Physics* **17**(16): 10093–10107. DOI: <http://dx.doi.org/10.5194/acp-17-10093-2017>.
- Camalier, L, Cox, W, Dolwick, P.** 2007. The effects of meteorology on ozone in urban areas and their use in assessing ozone trends. *Atmospheric Environment* **41**(33). DOI: <http://dx.doi.org/10.1016/j.atmosenv.2007.04.061>.
- Carpenter, A, Quispe-Agnoli, M.** 2015. A comparison of economic and social implications of rapid urbanization in Lima and Santiago de Chile. *Perspectives on Global Development and Technology*. DOI: <http://dx.doi.org/10.1163/15691497-12341358>.
- Cavanaugh, JE, Neath, AA.** 2019. *The Akaike information criterion: Background, derivation, properties, application, interpretation, and refinements*. Wiley Interdisciplinary Reviews: Computational Statistics. DOI: <http://dx.doi.org/10.1002/wics.1460>.
- Comisión Económica para América Latina y el Caribe/Organización Internacional del Trabajo.** 2020. El trabajo en tiempos de pandemia: Desafíos frente a la enfermedad por COVID-19. *Coyuntura Laboral en América Latina y el Caribe* **22**: 1–51.

- Chang, SC, Lee, CT.** 2007. Secondary aerosol formation through photochemical reactions estimated by using air quality monitoring data in Taipei City from 1994 to 2003. *Atmospheric Environment* **41**(19): 4002–4017. DOI: <http://dx.doi.org/10.1016/j.atmosenv.2007.01.040>.
- Connerton, P, de Assunção, JV, de Miranda, RM, Slovic, AD, Pérez-Martínez, PJ, Ribeiro, H.** 2020. Air quality during covid-19 in four megacities: Lessons and challenges for public health. *International Journal of Environmental Research and Public Health* **17**(14). DOI: <http://dx.doi.org/10.3390/ijerph17145067>.
- de Andrade, MF, Kumar, P, de Freitas, ED, Ynoue, RY, Martins, J, Martins, LD, Nogueira, T, Perez-Martínez, P, de Miranda, RM, Albuquerque, T, Gonçalves, FL.** 2017. Air quality in the megacity of São Paulo: Evolution over the last 30 years and future perspectives. *Atmospheric Environment* **159**: 66–82. DOI: <http://dx.doi.org/10.1016/j.atmosenv.2017.03.051>.
- East, J, Montealegre, JS, Pachon, JE, Garcia-Menendez, F.** 2021. Air quality modeling to inform pollution mitigation strategies in a Latin American megacity. *Science of the Total Environment* **776**. DOI: <http://dx.doi.org/10.1016/j.scitotenv.2021.145894>.
- Friedman, JH.** 2001. Greedy function approximation: A gradient boosting machine. *Annals of Statistics* **29**(5). DOI: <http://dx.doi.org/10.1214/aos/1013203451>.
- Fujita, EM, Stockwell, WR, Campbell, DE, Keislar, RE, Lawson, DR.** 2003. Evolution of the magnitude and spatial extent of the weekend ozone effect in California's South Coast Air Basin, 1981–2000. *Journal of the Air & Waste Management Association* **53**(7): 802–815. DOI: <http://dx.doi.org/10.1080/10473289.2003.10466225>.
- Gallardo, L, Barraza, F, Ceballos, A, Galleguillos, M, Huneeus, N, Lambert, F, Ibarra, C, Munizaga, M, O'Ryan, R, Osses, M, Tolvett, S.** 2018. Evolution of air quality in Santiago: The role of mobility and lessons from the science-policy interface. *Elementa: Science of the Anthropocene* **6**(1): 38. DOI: <http://dx.doi.org/10.1525/elementa.293>.
- Garschagen, M, Romero-Lankao, P.** 2015. Exploring the relationships between urbanization trends and climate change vulnerability. *Climatic Change* **133**(1). DOI: <http://dx.doi.org/10.1007/s10584-013-0812-6>.
- Gaubert, B, Bouarar, I, Doumbia, T, Liu, Y, Stavrou, T, Deroubaix, A, Darras, S, Elguindi, N, Granier, C, Lacey, F, Müller, JF.** 2021. Global changes in secondary atmospheric pollutants during the 2020 COVID-19 pandemic. *Journal of Geophysical Research: Atmospheres* **126**(8). DOI: <http://dx.doi.org/10.1029/2020JD034213>.
- Gkatzelis, GI, Gilman, JB, Brown, SS, Eskes, H, Gomes, AR, Lange, AC, McDonald, BC, Peischl, J, Petzold, A, Thompson, CR, Kiendler-Scharr, A.** 2021. The global impacts of COVID-19 lockdowns on urban air pollution: A critical review and recommendations. *Elementa*. DOI: <http://dx.doi.org/10.1525/elementa.2021.00176>.
- Goldstein, AH, Galbally, IE.** 2007. Known and unexplored organic constituents in the earth's atmosphere. *Environmental Science and Technology*. DOI: <http://dx.doi.org/10.1021/es072476p>.
- Guzman, LA, Bocarejo, JP.** 2017. Urban form and spatial urban equity in Bogota, Colombia. *Transportation Research Procedia* **25**. DOI: <http://dx.doi.org/10.1016/j.trpro.2017.05.345>.
- Holben, BN, Eck, TF, Slutsker, I, Tanré, D, Buis, JP, Setzer, A, Vermote, E, Reagan, JA, Kaufman, YJ, Nakajima, T, Lavenu, F, Jankowiak, I, Smirnov, A.** 1998. AERONET—A federated instrument network and data archive for aerosol characterization. *Remote Sensing of Environment* **66**(1). DOI: [http://dx.doi.org/10.1016/S0034-4257\(98\)00031-5](http://dx.doi.org/10.1016/S0034-4257(98)00031-5).
- Huneeus, N, Schulz, M, Balkanski, Y, Griesfeller, J, Prospero, J, Kinne, S, Bauer, S, Boucher, O, Chin, M, Dentener, F, Diehl, T.** 2011. Global dust model intercomparison in AeroCom phase I. *Atmospheric Chemistry and Physics* **11**(15). DOI: <http://dx.doi.org/10.5194/acp-11-7781-2011>.
- Ibarra-Espinosa, S, Ynoue, RY, O'sullivan, S, Pebesma, E, de Fátima Andrade, M, Osses, M.** 2018. VEIN v0.2.2: An R package for bottom-up vehicular emissions inventories. *Geoscientific Model Development* **11**(6). DOI: <http://dx.doi.org/10.5194/gmd-11-2209-2018>.
- Ibarra-Espinosa, S, Ynoue, RY, Ropkins, K, Zhang, X, de Freitas, ED.** 2020. High spatial and temporal resolution vehicular emissions in south-east Brazil with traffic data from real-time GPS and travel demand models. *Atmospheric Environment* **222**. DOI: <http://dx.doi.org/10.1016/j.atmosenv.2019.117136>.
- Instituto Nacional de Estadísticas.** 2017. Census 2017. Available at <http://www.censo2017.cl>.
- Jacques-Coper, M, Veloso-Aguila, D, Segura, C, Valencia, A.** 2021. Intraseasonal teleconnections leading to heat waves in central Chile. *International Journal of Climatology*. DOI: <http://dx.doi.org/10.1002/joc.7096>.
- Javid, A, Creutzig, F, Bamberg, S.** 2020. Determinants of low-carbon transport mode adoption: Systematic review of reviews. *Environmental Research Letters*. DOI: <http://dx.doi.org/10.1088/1748-9326/aba032>.
- Judd, LM, Al-Saadi, JA, Szykman, JJ, Valin, LC, Janz, SJ, Kowalewski, MG, Eskes, HJ, Pepijn Veefkind, J, Cede, A, Mueller, M, Gebetsberger, M.** 2020. Evaluating Sentinel-5P TROPOMI tropospheric NO<sub>2</sub> column densities with airborne and Pandora spectrometers near New York City and Long Island Sound. *Atmospheric Measurement Techniques* **13**(11). DOI: <http://dx.doi.org/10.5194/amt-13-6113-2020>.
- Kavassalis, SC, Murphy, JG.** 2017. Understanding ozone-meteorology correlations: A role for dry deposition. *Geophysical Research Letters* **44**(6). DOI: <http://dx.doi.org/10.1002/2016GL071791>.



- Kelly, FJ, Zhu, T.** 2016. Transport solutions for cleaner air. *Science*. DOI: <http://dx.doi.org/10.1126/science.aaf3420>.
- Kroll, JH, Heald, CL, Cappa, CD, Farmer, DK, Fry, JL, Murphy, JG, Steiner, AL.** 2020. The complex chemical effects of COVID-19 shutdowns on air quality. *Nature Chemistry*. DOI: <http://dx.doi.org/10.1038/s41557-020-0535-z>.
- The Lancet.** 2020. COVID-19 in Brazil: "So what?" *The Lancet*. DOI: [http://dx.doi.org/10.1016/S0140-6736\(20\)31095-3](http://dx.doi.org/10.1016/S0140-6736(20)31095-3).
- Le, T, Wang, Y, Liu, L, Yang, J, Yung, YL, Li, G, Seinfeld, JH.** 2020. Unexpected air pollution with marked emission reductions during the COVID-19 outbreak in China. *Science* **369**(6504). DOI: <http://dx.doi.org/10.1126/science.abb7431>.
- Mangones, SC, Jaramillo, P, Fischbeck, P, Rojas, NY.** 2019. Development of a high-resolution traffic emission model: Lessons and key insights from the case of Bogotá, Colombia. *Environmental Pollution* **253**. DOI: <http://dx.doi.org/10.1016/j.envpol.2019.07.008>.
- Menares, C, Gallardo, L, Kanakidou, M, Seguel, R, Huneus N.** 2020. Increasing trends (2001–2018) in photochemical activity and secondary aerosols in Santiago, Chile. *Tellus, Series B: Chemical and Physical Meteorology* **72**(1). DOI: <http://dx.doi.org/10.1080/16000889.2020.1821512>.
- Mendez-Espinosa, JF, Belalcazar, LC, Morales Betancourt, R.** 2019. Regional air quality impact of northern South America biomass burning emissions. *Atmospheric Environment* **203**. DOI: <http://dx.doi.org/10.1016/j.atmosenv.2019.01.042>.
- Mendez-Espinosa, JF, Rojas, NY, Vargas, J, Pachón, JE, Belalcazar, LC, Ramírez, O.** 2020. Air quality variations in Northern South America during the COVID-19 lockdown. DOI: <http://dx.doi.org/10.1016/j.scitotenv.2020.141621>.
- Molnar, C.** 2022. Interpretable machine learning. A guide for making black box models explainable. Available at <https://christophm.github.io/interpretable-ml-book/>.
- Nakada, LYK, Urban, RC.** 2020. COVID-19 pandemic: Impacts on the air quality during the partial lockdown in São Paulo state, Brazil. *Science of the Total Environment* **730**. DOI: <http://dx.doi.org/10.1016/j.scitotenv.2020.139087>.
- Nogueira, T, de Souza, KF, Fornaro, A, de Fatima Andrade, M, de Carvalho, LRF.** 2015. On-road emissions of carbonyls from vehicles powered by biofuel blends in traffic tunnels in the Metropolitan Area of Sao Paulo, Brazil. *Atmospheric Environment* **108**: 88–97.
- Ordóñez, C, Garrido-Perez, JM, García-Herrera, R.** 2020. Early spring near-surface ozone in Europe during the COVID-19 shutdown: Meteorological effects outweigh emission changes. *Science of the Total Environment* **747**. DOI: <http://dx.doi.org/10.1016/j.scitotenv.2020.141322>.
- Osses, A, Gallardo, L, Faundez, T.** 2013. Analysis and evolution of air quality monitoring networks using combined statistical information indexes. *Tellus, Series B: Chemical and Physical Meteorology* **65**: 1–17. DOI: <http://dx.doi.org/10.3402/tellusb.v65i0.19822>.
- Parrish, DD, Ryerson, TB, Holloway, JS, Trainer, M, Fehsenfeld, FC.** 1999. New directions: Does pollution increase or decrease tropospheric ozone in Winter-Spring? *Atmospheric Environment* **33**(30). DOI: [http://dx.doi.org/10.1016/S1352-2310\(99\)00253-8](http://dx.doi.org/10.1016/S1352-2310(99)00253-8).
- Porter, WC, Heald, CL.** 2019. The mechanisms and meteorological drivers of the summertime ozone-temperature relationship. *Atmospheric Chemistry and Physics* **19**(21). DOI: <http://dx.doi.org/10.5194/acp-19-13367-2019>.
- Rodríguez-Villamizar, LA, Belalcázar-Ceron, LC, Fernández-Niño, JA, Marín-Pineda, DM, Rojas-Sánchez, OA, Acuña-Merchán, LA, Ramírez-García, N, Mangones-Matos, SC, Vargas-González, JM, Herrera-Torres, J, Agudelo-Castañeda, DM.** 2021. Air pollution, sociodemographic and health conditions effects on COVID-19 mortality in Colombia: An ecological study. *Science of the Total Environment* **756**. DOI: <http://dx.doi.org/10.1016/j.scitotenv.2020.144020>.
- Romero, H, Vásquez, A, Fuentes, C, Salgado, M, Schmidt, A, Banzhaf, E.** 2012. Assessing urban environmental segregation (UES). The case of Santiago de Chile. *Ecological Indicators* **23**. DOI: <http://dx.doi.org/10.1016/j.ecolind.2012.03.012>.
- Salvo, A, Brito, J, Artaxo, P, Geiger, FM.** 2017. Reduced ultrafine particle levels in São Paulo's atmosphere during shifts from gasoline to ethanol use. *Nature Communications* **8**(1). DOI: <http://dx.doi.org/10.1038/s41467-017-00041-5>.
- Salvo, A, Geiger, FM.** 2014. Reduction in local ozone levels in urban São Paulo due to a shift from ethanol to gasoline use. *Nature Geoscience* **7**(6): 450.
- Schuch, D, de Freitas, ED, Espinosa, SI, Martins, LD, Carvalho, VSB, Ramin, BF, Silva, JS, Martins, JA, de Fatima Andrade, M.** 2019. A two decades study on ozone variability and trend over the main urban areas of the São Paulo state, Brazil. *Environmental Science and Pollution Research* **26**(31). DOI: <http://dx.doi.org/10.1007/s11356-019-06200-z>.
- Schuster, GL, Dubovik, O, Holben, BN.** 2006. Angstrom exponent and bimodal aerosol size distributions. *Journal of Geophysical Research Atmospheres* **111**(7). DOI: <http://dx.doi.org/10.1029/2005JD006328>.
- Seguel, RJ, Gallardo, L, Fleming, ZL, Landeros, S.** 2020. Two decades of ozone standard exceedances in Santiago de Chile. *Air Quality, Atmosphere & Health*. DOI: <http://dx.doi.org/10.1007/s11869-020-00822-w>.
- Seguel, RJ, Morales, S, RGE, Leiva, G, MA.** 2012. Ozone weekend effect in Santiago, Chile. *Environmental Pollution* **162**. DOI: <http://dx.doi.org/10.1016/j.envpol.2011.10.019>.
- Shi, Z, Song, C, Liu, B, Lu, G, Xu, J, van Vu, T, Elliott, RJR, Li, W, Bloss, WJ, Harrison, RM.** 2021. Abrupt but smaller than expected changes in surface air

- quality attributable to COVID-19 lockdowns. *Science Advances* **7**(3). DOI: <http://dx.doi.org/10.1126/sciadv.abd6696>.
- Siciliano, B, Carvalho, G, da Silva, CM, Arbilla, G.** 2020. The impact of COVID-19 partial lockdown on primary pollutant concentrations in the atmosphere of Rio de Janeiro and São Paulo Megacities (Brazil). *Bulletin of Environmental Contamination and Toxicology* **105**(1). DOI: <http://dx.doi.org/10.1007/s00128-020-02907-9>.
- Silva Júnior, RS da, Oliveira, MGL de, Andrade, M de F.** 2009. Weekend/weekday differences in concentrations of ozone, nox, and non-methane hydrocarbon in the metropolitan area of São Paulo. *Revista Brasileira de Meteorologia* **24**(1). DOI: <http://dx.doi.org/10.1590/s0102-77862009000100010>.
- Sokhi, RS, Singh, V, Querol, X, Finardi, S, Targino, AC, Andrade M de, F, Pavlovic, R, Garland, RM, Masagué, J, Kong, S, Baklanov, A.** 2021. A global observational analysis to understand changes in air quality during exceptionally low anthropogenic emission conditions. *Environment International* **157**. DOI: <http://dx.doi.org/10.1016/j.envint.2021.106818>.
- Solberg, S, Walker, SE, Schneider, P, Guerreiro, C.** 2021. Quantifying the impact of the covid-19 lockdown measures on nitrogen dioxide levels throughout Europe. *Atmosphere* **12**(2). DOI: <http://dx.doi.org/10.3390/atmos12020131>.
- Tolvett-Caro, S, Henríquez, P, Osses, M.** 2016. Análisis de variables significativas para la generación de un inventario de emisiones de fuentes móviles y su proyección. *Ingeniare* **24**: 32–39. DOI: <http://dx.doi.org/10.4067/S0718-33052016000500005>.
- Toro, AR, Catalán, F, Urdanivia, FR, Rojas, JP, Manzano, CA, Seguel, R, Gallardo, L, Osses, M, Pantoja, N, Leiva-Guzman, MA.** 2021. Air pollution and COVID-19 lockdown in a large South American city: Santiago Metropolitan Area, Chile. *Urban Climate* **36**. DOI: <http://dx.doi.org/10.1016/j.uclim.2021.100803>.
- United Nations Department of Economic and Social Affairs, Population Division.** 2019. *World urbanization prospects: The 2018 revision*. New York, NY. DOI: <http://dx.doi.org/10.18356/b9e995fe-en>.
- van Geffen, J, Folkert Boersma, K, Eskes, H, Sneep, M, ter Linden, M, Zara, M, Pepijn Veefkind, J.** 2020. S5P TROPOMI NO<sub>2</sub> slant column retrieval: Method, stability, uncertainties and comparisons with OMI. *Atmospheric Measurement Techniques* **13**(3). DOI: <http://dx.doi.org/10.5194/amt-13-1315-2020>.
- Vara-Vela, A., Andrade, MF, Kumar, P, Ynoue, RY, Muñoz, AG.** 2016. Impact of vehicular emissions on the formation of fine particles in the Sao Paulo metropolitan area: A numerical study with the WRF-Chem model. *Atmospheric Chemistry and Physics* **16**(2). DOI: <http://dx.doi.org/10.5194/acp-16-777-2016>.
- Verhoelst, T, Compennolle, S, Pinardi, G, Lambert, JC, Eskes, HJ, Eichmann, KU, Fjæraa, AM, Granville, J, Niemeijer, S, Cede, A, Tiefengraber, M.** 2021. Ground-based validation of the Copernicus Sentinel-5P TROPOMI NO<sub>2</sub> measurements with the NDACC ZSL-DOAS, MAX-DOAS and Pandonia global networks. *Atmospheric Measurement Techniques* **14**(1). DOI: <http://dx.doi.org/10.5194/amt-14-481-2021>.
- Wood, SN.** 2017. *Generalized additive models: An introduction with R*. London, UK: Chapman and Hall/CRC.

**How to cite this article:** Seguel, RJ, Gallardo, L, Osses, M, Rojas, NY, Nogueira, T, Menares, C, de Fatima Andrade, M, Belalcázar, LC, Carrasco, P, Eskes, H, Fleming, ZL, Huneus, N, Ibarra-Espinosa, S, Landulfo, E, Leiva, M, Mangones, SC, Morais, FG, Moreira, GA, Pantoja, N, Parraguez, S, Rojas, JP, Rondanelli, R, da Silva Andrade, I, Toro, R, Yoshida, AC. 2022. Photochemical sensitivity to emissions and local meteorology in Bogotá, Santiago, and São Paulo: An analysis of the initial COVID-19 lockdowns. *Elementa: Science of the Anthropocene* **10**(1). DOI: <https://doi.org/10.1525/elementa.2021.00044>

**Domain Editor-in-Chief:** Detlev Helmig, Boulder AIR LLC, Boulder, CO, USA

**Associate Editor:** Jochen Stutz, Department of Atmospheric and Oceanic Sciences, University of California, Los Angeles, CA, USA

**Knowledge Domain:** Atmospheric Science

**Published:** May 12, 2022    **Accepted:** April 8, 2022    **Submitted:** June 14, 2021

**Copyright:** © 2022 The Author(s). This is an open-access article distributed under the terms of the Creative Commons Attribution 4.0 International License (CC-BY 4.0), which permits unrestricted use, distribution, and reproduction in any medium, provided the original author and source are credited. See <http://creativecommons.org/licenses/by/4.0/>.

